MODELLING CROSS-LAMINATED TIMBER FLOORS IN DYNAMIC ANALYSIS
Eigenfrequency prediction

JOHANNES WETTERHOLT

Master's Dissertation

MODELLING CROSS-LAMINATED TIMBER FLOORS IN DYNAMIC ANALYSIS
Eigenfrequency prediction

JOHANNES WETTERHOLT

Abstract

In the late 1990s cross-laminated timber (CLT) was developed. The development of CLT was a project aimed to produce a structural product that could compete with the concrete industry and contribute to a reduced effect on the environment, due to the low environmental impact of timber in relation to other building materials. CLT elements are usually constructed as panels which contain multiple layers of laminations, where every second layer is oriented in a 90-degree angle to adjacent layers. The layup and the youth of CLT implies that design approaches for timber structures available today are not fully applicable to CLT. The final design of wooden floor slabs is most often governed by serviceability limit state requirements, often relating to deflection and vibration in the vertical direction. An employed method to analyse the vibration susceptibility of wooden floor slabs is through a numerical analysis, which is executed with software that uses the finite element method. To produce models that have the same characteristic behaviour as a real floor design is of great importance. Research concerning how to create appropriate models of CLT floor slabs has been performed, although, more research is necessary to be able to determine modelling features regarding support conditions, material properties and other modelling options.

In this Master's dissertation, an evaluation of how different modelling options affect the modal response up to 80 Hz of a CLT floor slab is presented. The necessary level of detail of the structure of a CLT floor and the possibility to simplify the description of the material properties and still obtaining relevant results in terms of modal behaviour was evaluated. Four finite element models were assembled with different levels of detail, based on a selected CLT floor element. An analytical evaluation was performed, based on a derivation of the fundamental frequency for a simply supported beam considered as a continuous media, which also is given in the recommended design codes (Eurocode 5).

The most advanced model that was created is three-dimensional and includes five layers, all individual laminations and a gap of 0.2 millimetres between the laminations. The second model is three-dimensional and each of the five layers of laminations are modelled as one unit; the gap is excluded. The third model, is two-dimensional and includes all the five layers. The fourth model, is a two-dimensional plate where no individual layers or laminations are modelled. In addition, an analytic model was created where the fundamental frequency was evaluated.

The result of the finite element analyses shows that there are great similarities of the modal response between the three most advanced models that include the orthotropic characteristics, while the fourth model and the models with modified material parameters diverge. This indicates that the individual layers of laminations and the orthotopic characteristics are necessary to include in the modelling to produce an accurate model of a CLT floor when analysing modal response up to 80 Hz. The individual laminations are, however, not necessary to model. The use of isotropic characteristics did not give satisfactory results.

If only the fundamental frequency is of interest, a simple one-dimensional model is sufficient to predict accurate modal behaviour. The finite element models were able to produce an accurate prediction of the fundamental frequency, the fourth model (the two-dimensional plate model) required some tuning of the material properties to give an accurate response.

Sammanfattning

I slutet av 90-talet utvecklades produkten korslimmat trä, KL-trä. Framtagningen av KL-trä var ett projekt för att framställa ett byggnadsmaterial med avseende att kunna konkurrera med betongindustrin och därigenom bidra till en lägre miljöpåverkan, då trä har en låg påverkan på miljön i förhållande till många andra konstruktionsmaterial. KL-träelement är vanligtvis konstruerade som plattor och har en uppbyggnad av flertalet lager av lameller, där vartannat lager är riktat 90 grader i förhållande till intilliggande. De aktuella dimensioneringsmetoderna för träkonstruktioner behöver utvärderas om de är applicerbara för KL-träelement, då lamelluppbyggnaden medför andra egenskaper. Vid dimensionering av just träbjälklagsel-ement är ofta brukgränstillståndet med avseende på nedböjning och vibrationer det som är avgörande för de slutliga dimensionerna. En ofta använd metod för att analysera bjälkagsvibrationer är att använda numerisk analys, vilket genomförs med hjälp av finita element program. Att skapa modeller som har samma karakteristiska beteende som ett verkligt golv är av stor betydelse för dimensioneringsprocessen. Forskning har genomförts kring modellering av KL-träbjälklag men fortfarande finns det oklarheter angående antagande som rör upplagsvilkor, materialdata och andra modelleringsparameterar.

I detta examensarbete undersöks hur olika modelleringsval påverkar den modala responsen av ett KL-trä bjälklag upp till 80 Hz. Den nödvändiga detaljeringsnivån som krävs vid modellering av den inre strukturen av ett KL-trä bjälklag samt om det är möjligt att förenkla matrialegenskaperna och behålla det modala beteendet utvärderas. Fyra finita element modeller med olika detaljeringsnivå skapas, med utgångspunkt i ett och samma standardiserade KL-trä bjälklag. En analytisk undersökning som baseras på en härledning av den första resonansfrekvensen och som också finns omnämnd i de svenska dimensioneringsrekommendationerna (Eurocode) för träbjälklag utförs av bjälklaget .

Den mest avancerande modellen som skapades är tredimensionell och inkluderar alla individuella lameller i de fem lager som är studerade samt ett avstånd mellan lamellerna på 0,2 millimeter. Den andra modellen är också tredimensionell med förenklingen att alla lameller i varje separat skikt verkar som en individuell platta, alltså är inga mellanrum medräknade. Den tredje modellen är tvådimensionell och innefattar de fem separata lagrena där materialparametrarna anges. Den sista och minst detaljerade modellen är en tvådimensionell platta som summerar alla lameller i ett skikt. En analytisk model görs också där första resonansfrekvensen analyseras.

I resultatet av finita elementanalyserna kan man se stora likheter i det modala beteendet hos de tre mest avancerade modellerna medan den fjärde avviker från resultaten. Detta antyder att, för att återskapa en modell som fångar det modala beteendet upp till omkring 80 Hz, måste de olika lamellskikten samt de ortotropa materialegenskaperna modelleras. Individuella lameller behöver dock inte tas hänsyn till. Försök gjordes för att återskapa det modala beteendet med isotropa materialparametrar men detta visade sig ge otillfredställande resultat.

Om endast den första resonansfrekvensen är av intresse kan en endimensionell modell användas för att skapa en godtagbar uppskattning av den modala responsen. Samtliga fem modeller kunde återskapa den första resonansfrekvensen. Den tvådimensionella modellen som modelleras som en platta kräver dock att materialegenskaperna anpassas för att återskapa beteendet av första resonansfrekvensen.

Preface

This Master's dissertation was carried out at the Division of Structural Mechanics at the Faculty of Engineering, Lund University. The work was performed during the spring semester 2019.

Lund, May 2019
Johannes Wetterholt

Notation

General notations

$\sum (\ )$	sum of ( )
$\lvert \ (\ ) \ \rvert$	absolute value of ( )
$det[\ ]$	determinant of [ ]
$(\ )^{\mathrm{T}}$	transpose of ( )

Roman upper case letters

A	area
A_n	constant
B_n	constant
C_1	constant
C_2	constant
C_3	constant
C_4	constant
$\mathbf{C}$	damping matrix
D	stiffness parameter
$\mathbf{D}$	constitutive matrix
E	modulus of elasticity, Young's modulus
F	shear force
G	modulus of rigidity, shear modulus
$G_{9090,x}$	shear rolling stiffness
I	second moment of inertia
I_{ef}	effective second moment of inertia
$\mathbf{K}$	stiffness matrix
M	moment
$\mathbf{M}$	mass matrix
P	concentrated static load
T_n	natural period of vibration

Roman lower case letters

a	constant
b	width
c	damping coefficient
f_c	damper force
f_n	natural frequency

$f_{n,i}$	eigenfrequency of number i
f_s	spring force
f_1	fundamental frequency, first natural frequency
h	height
k	spring stiffness
l	length
l_{ref}	length modified with the column effective length factor
m	mass
n	order number
n_{40}	number of first-order modes with frequencies up to 40 Hz
$\mathbf{p}$	concentrated static load vector
q_n	modal coordinates
t	time
t_i	thickness of lamination layer i
u	displacement
u_0	initial displacement
$\mathbf{u}$	displacement vector
$\dot{u}$	velocity
$\dot{u}_0$	initial velocity
$\dot{\mathbf{u}}$	velocity vector
$\ddot{u}$	acceleration
$\ddot{\mathbf{u}}$	acceleration vector
v	impulse velocity response
w	maximum instantaneous vertical deflection
z	lever arm

Greek letters

α	wavelength of a sinusoidal wave
β	column effective length factor
γ	gamma-factor, reduction factor
ε	strain
$\boldsymbol{\varepsilon}$	strain vector
ζ	modal damping ratio
ν	Poisson's ratio
ρ	density
σ	stress
$\boldsymbol{\sigma}$	stress vector
ϕ_n	natural mode
φ	phase
ψ	reduction factor
ω	angular frequency
ω_n	natural angular frequency

Contents

1 Introduction

1.1 Background

Floor slabs may be constructed in multiple ways and with different materials, depending on, for example, the loading situation and the requirements placed on the finished floor slab. Materials that normally are used for the load-bearing part of the floor are concrete, wood or composites of either steel/concrete or wood/concrete. Wooden floor elements may be constructed in different ways. In the late 1990s when cross-laminated timber (CLT) panels were developed, it entered the building industry and has continued to expand ever since (Borgström and Fröbel, 2017). CLT panels are constructed of multiple stacked layers of laminations, where every second layer is oriented in a 90-degree angle in relation to adjacent layers, see Figure 1.1. The ply layup contributes to a stiff structure in relation to more traditional wooden floor elements.
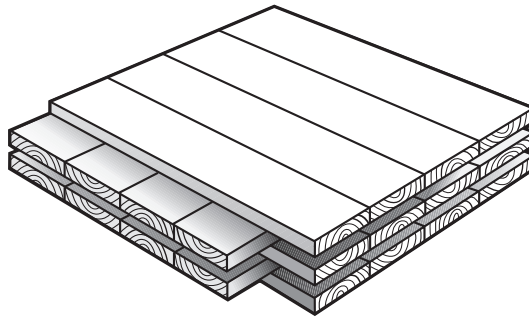

Figure 1.1: An example of a CLT panel built up of five layers of laminations.

The usage of wood as a building material has through time mainly been for residential buildings. In Sweden, a ban on constructing wooden buildings over two stories was present to prevent and limit the damage of fires spreading between buildings within dense cities (Giang and Moroz, 2013). In the year 1994, the building restriction was lifted and ever since an increase in usage of wood as a construction material for multi-storey buildings has been seen.

Wood has advantages compared to other construction materials normally used for multi-storey buildings, such as steel and concrete. Wood has relatively high strength in relation to its cost and is an environmentally friendly and sustainable material (Borgström and Fröbel, 2017). Although there are some disadvantages of wood, the fact that wood is a natural material implies that its features come in a large variety, which results in an uncertainty of the material properties between individual samples. In some structural engineering aspects, the low mass of wood is a disadvantage. Lightweight building materials are in general susceptible to sound transmission and dynamic response. This may result in discomfort for the residents and users in terms of noise and annoying vibrations.

Floor slabs are designed for vertical and horizontal forces where the resulting dimen-

sions often are governed by the serviceability limit state (SLS) requirements, relating to deflection and vibration in the vertical direction (EN 1995-1-1, 2016). Wooden elements, which in general are slender with relatively low mass, are especially sensitive to dynamic loads. In EN 1995-1-1 (2016), an analytic design approach is given. The design approach includes a general evaluation of the fundamental frequency evaluated through one-dimensional beam-theory, evaluation of an impulse velocity response and the deflection of a 1.0 kN static point load.

Another widely used approach to evaluate wooden elements is through the finite element (FE) method. Numerical simulations have been shown to be applicable to simulate the response of structural elements, which has the effect that the amount of test on a real element can be reduced. Numerical simulations are employable to investigate how parametric variation in geometry and variation/uncertainties in material properties influences an element. An appropriate FE model that behaves like the actual floor is of great importance. Variety in material parameters, the level of detail of the modelled element and applied support condition may contribute to a crucial difference in the results during the design procedure. There is an interest of increasing the knowledge of how to model wooden floor slabs and determine what parameters that are of importance and what assumptions that can be made to reduce the error of the response between model and actual floor structure. The stiffness parameters of wood given in literature are related to uncertainties due to the fact that wood is a natural material. To be able to predict the dynamic behaviour of a wooden floor with a FE model most of the times some calibration of the stiffness parameters is required to achieve similar results as to an actual experimental testing floor. Bolmsvik et al. (2012) assigned material properties of CLT given in literature to a FE model and compared the dynamic response with an actual test structure. With some refining of the assigned properties to the FE model, a more accurate response was achieved.

In a study performed by Persson and Flodén (2018), the effect of material parameters on the vibroacoustic response of a wooden floor was investigated. Monte Carlo (MC) simulations were conducted to account for the natural variability in wood parameters and assigned to a FE model. In Persson and Flodén (2019), the floor model was further investigated regarding the effect of variability of material parameters. The vibroacoustic response was compared with measurement data and the FE model calibrated to achieve a time-efficient numerical analysis. By assigning the stochastic approach through MC simulations determined in the previous study it could be shown that the natural variation of wood has a marked effect on the vibroacoustic response. The stochastic approach employed provides knowledge of how to develop reliable numerical models which take the material uncertainties into account.

A study was performed by Qian et al. (2019) to evaluate the natural variation of the wooden properties in a CLT element and the relation between Young's moduli and shear moduli. A stochastic approach was used to quantify uncertainties of properties in different material orientations. Out of 100 MC simulations, the best combination of material parameters in comparison to a experimental test structure was selected to calibrate the FE CLT model with regards to dynamic response. The stochastic method seemed employable when analysing a CLT structure in vibration with a frequency up to 100 Hz.

In a study by Ussher et al. (2017), FE models were created and compared with experimental data of CLT floors collected from the University of New Brunswick. The analyses included variations of the dimensions of the CLT floor and multiple CLT elements connected by joints where modelled. The support conditions were also changed: simply supported along two opposite edges and the other side edges free, as well as, simply supported along all four edges. The study concluded that multiple different features, such as joints and support conditions, influence the dynamic response and that simplified analytical methods to determine the modal characteristic of CLT floors are unsatisfactory.

1.2   Aim and objective

The aim of this Master's dissertation is to identify what assumptions and simplifications that may be assumed when creating a FE model of a CLT floor slab and remain the possibility to predict the eigenfrequencies. The simplified FE models are compared to a more advanced model. A simplified model may be able to ease the design procedure of CLT slabs for engineers and reduce the computational cost during calculations. To achieve that, different FE models will be compared to establish the level of detail that is necessary to create a model without loss in accuracy. To be able to achieve the aim, the following objectives are specified:

- Investigate how different FE elements and meshes influence modal properties of a CLT floor.

- Evaluate if the recommended prediction method of the fundamental frequency of wooden floors is applicable to CLT floors.

- Identify possible similarities and differences in the frequency response between two-dimensional and three-dimensional FE models.

- Evaluate how the layered structure of laminations affects the eigenfrequencies of a modelled CLT floor.

- Evaluate if it is possible to simplify the layered composition of laminations in a CLT floor slab when predicting eigenfrequencies.

- Determine a strategy for modelling a CLT floor with isotropic material properties.

1.3   Method

The FE models will be created and analysed in the FE software Abaqus CAE, where the eigenfrequencies will be compared between the different models and evaluated. Four models will be analysed numerically, and in addition, an one-dimensional analytical model will be performed.

1.4   Limitations

The analyses in this dissertation are focusing on the numerical modelling of CLT floors with no comparison to a real test floor. One set of dimensions of the floor slab is chosen and is not changed throughout the investigation, both the total dimensions of the floor and the dimensions of the internal laminations are kept constant. One floor element is analysed and no joints are included. The wood material is modelled as orthotropic, with exception to the analyses replicating the orthotropic features with isotropic properties. The laminations are modelled as homogeneous, meaning that the individual annual rings, knots and similar features are not taken into consideration. The orthotropic material directions are considered as homogeneous for all laminations and are not changed due to the curvature of the annual rings in the cross-section of the laminations. The strains caused by human walking and other dynamic loads occurring on the floor are assumed to be relatively small and therefore analysed according to a linear elastic behaviour.

1.5   Disposition

Below, a short resume of the content of each chapter is given:

Chapter 2 includes a description of the mechanical properties of wood and CLT of relevance for this dissertation. The natural variation of wood and its orthotropic characteristics are introduced and relevant background regarding linear elasticity and engineering constants is presented. Finally, some brief history and the assemblage of CLT panels are presented and what consequences the CLT structure results in for the mechanical properties.

Chapter 3 describes two methods to analyse the dynamics of structural elements. The discrete method is first presented, which is used in the FE analysis. Then, an equation to predict the eigenfrequencies for a floor considered as an one-dimensional beam and as a continuous media is derived.

In **Chapter 4**, guidelines given in the literature for design of vibrations of floor elements and material properties are presented. An one-dimensional analysis of the CLT floor model according to Eurocode is performed.

Chapter 5 includes all information and the assumptions about the four FE models and the results of the FE analyses. Each model is first presented separately, starting with the most detailed model and ending with the least detailed. Finally, a summary of the results is given.

In **Chapter 6** the results are compared, analysed and discussed. Similarities and differences between the models are established.

Chapter 7 contain conclusions drawn from the analysed results, and what studies that may be of interest in the future to further contribute with knowledge on the subject are given.

2   Mechanical properties of wood

In this chapter, the mechanical properties of wood considered for use as a construction material are described. First, a brief introduction of the general features of wood and the principal material directions are given. Then, the linear elastic properties and the engineering stiffness parameters are presented. Finally, CLT panels are introduced and how their assemblage affected the mechanical properties is discussed.

2.1   Introduction

Wood is a natural material and the material properties between different samples and populations may have a large variation (Johansson, 2016). The material properties are greatly influenced by the circumstances of the surrounding environment during the growth period of the tree. For example, conditions as moisture, soil content, growing space and speed influences the material. During the growth of the tree anomalies form in the wood structure, for example, branches results in knots and spiral grain give a flexible structure against wind loads. In general, wood is considered as an inhomogeneous material. The features of wood are although dependent on which scale they are being analysed in (Dahl, 2009). The smaller the scale of a sample that is considered, the less anomalies and imperfections are included. The structural level of the problem at hand governs on which scale that the material properties should be determined from. Even if the properties of different scales are determined separately, they are directly related to each other and influences properties on other levels. The scales can be categorized into different levels, depending on circumstances and preferences. Below, the features of wood are separated into four typical categories dependent on the scale of observation; massive; macro; meso; and micro scale.

The massive scale describes wood which includes anomalies as knots, spiral grain, cracks and other similar characteristics in a global perspective. The mechanical properties of structural timber classified in the massive scale are often determined on element level and not on a material level, due to the amount of defects.

The macro scale includes all features that can be observed by the naked eye (Dahl, 2009). Bark, cambium, sapwood, heartwood and the annual rings are considered in this scale, see Figure 2.1. The cambium is defined as the only cells capable of cell division and produces bark as well as new sapwood (Johansson, 2016). The sapwood transports liquids and nutrients between the ground and the crown of the tree. As the tree grows and produces new rings of sapwood, the inner cells convert into heartwood, the cells become thicker, the density increases and the water content decreases. The heartwood in most tree species has a darker colour than the sapwood. The pith is located at the centre of the annual rings and represents the first season of growth. The thickness of the annual rings are dependent on the seasonal growth. The pattern of annual rings on cut structural timber can be used to determine principal material directions and

planes. How the annual rings and the principal material directions affect the properties of wooden building components are further described in Section 2.2. The macro scale is most often used when defining the material properties of structural timber.
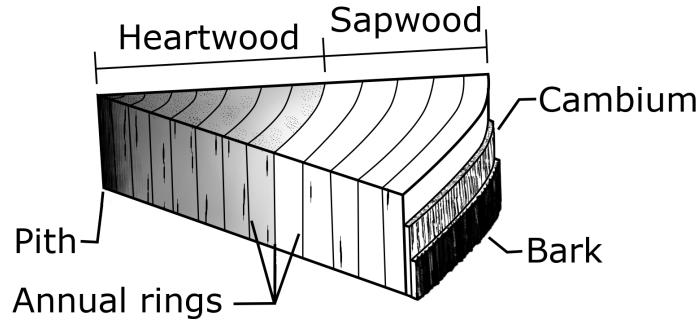

Figure 2.1: The internal structure of a tree and the components considered at the macro scale of wood; bark; cambium; sapwood; heartwood; pith; and annual rings.

The meso scale focus on the annual rings and how the growth varies between different seasons (Dahl, 2009). The season dependent growth is referred to as earlywood and latewood. Earlywood develops during the spring and is less dense than the latewood, which grows during the summer.

The micro scale is down on the cell structure of wood. It describes the function of the individual cell in the different sections of the wood trunk and how it is shaped and built to contribute to the different features as transportation of liquids and nutrients.

2.2 Orthotropic behaviour

When defining material characteristics internal organization of the material is identified (Bodig and Jayne, 1982). Most materials contain some symmetry features that makes it possible to simplify the mathematical description of their behaviour. A material with directional properties but no symmetry planes is defined as anisotropic, while a material with no directional properties nor symmetry planes or an infinite number of symmetry planes is classified as isotropic. Wood is usually considered as an orthotropic material and is defined as a material with the characteristics of three perpendicular symmetry planes (Green et al., 1999). The directions of the three symmetry planes are defined with regard to the orientation of the annual rings and are; longitudinal; radial; and tangential. The longitudinal direction is parallel to the grain of the wood, the radial direction is in the normal direction of the annual rings and perpendicular to the grain, and the tangential direction is perpendicular to the grain and in the tangent direction of the annual rings, see Figure 2.2.

the radial direction is in the normal direction of the annual rings and perpendicular to the grain
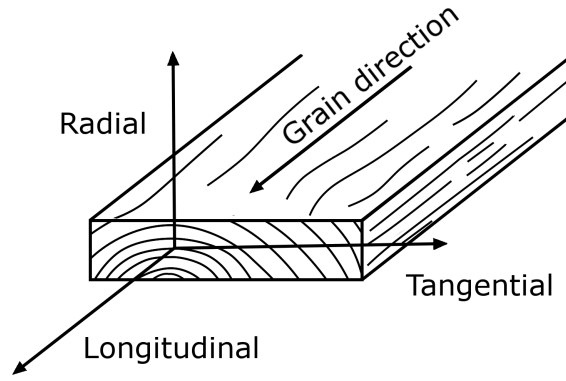
Figure 2.2: The three principal material directions; longitudinal; radial; and tangential showed in relation to a piece of structural timber.

2.2.1 Linear elastic orthotropy

All materials that are affected by any kind of force will deform from its original state. If the recovery of the material is instantaneous and complete the material behaviour is said to be elastic (Bodig and Jayne, 1982). No material is completely elastic in its behaviour, but some may be approximated to be so and especially if the deformations are relatively small. For some materials the relationship between deformation (strain) and stress is linear, in one dimension these materials can be expressed with Hooke's law (Ottosen and Petersson, 1992), see Equation 2.1. Hooke's law describes the stress (σ) as a linear function of the strain (ε). Where, the constant proportionality is expressed by the material constant E, also known as the modulus of elasticity or Young's modulus.

$$\sigma = E\varepsilon \tag{2.1}$$

For materials with linear elastic characteristics, the stress and strain may be described with several components (Ottosen and Petersson, 1992). A material analysed in multiple dimensions make use of stress and strain in different planes and how they affect each other, and the total is calculated by superposition of the stress and strain components. The stresses are then given by the vector $\boldsymbol{\sigma}$, the strains by the vector $\boldsymbol{\varepsilon}$ and the stiffness parameters are given in the constitutive matrix $\mathbf{D}$. These three quantities are related accordingly to Equation 2.2, which occasionally is referred to as Hooke's generalized law. $\boldsymbol{\sigma}$ and $\boldsymbol{\varepsilon}$ are of size 6×1 and $\mathbf{D}$ of size 6×6.

$$\boldsymbol{\sigma} = \mathbf{D}\boldsymbol{\varepsilon} \tag{2.2}$$

The constitutive matrix contains 36 different coefficients, but due to the number of symmetry planes within a material the coefficients can be reduced (Ottosen and Petersson, 1992). For an orthotropic material a reduction to nine independent coefficients can be performed, which results in the following constitutive matrix:

$$\mathbf{D} = \begin{bmatrix} D_{11} & D_{12} & D_{13} & 0 & 0 & 0 \\ D_{21} & D_{22} & D_{23} & 0 & 0 & 0 \\ D_{31} & D_{32} & D_{33} & 0 & 0 & 0 \\ 0 & 0 & 0 & D_{44} & 0 & 0 \\ 0 & 0 & 0 & 0 & D_{55} & 0 \\ 0 & 0 & 0 & 0 & 0 & D_{66} \end{bmatrix} \tag{2.3}$$

7

where, $D_{12} = D_{21}$, $D_{13} = D_{31}$ and $D_{23} = D_{32}$, since $\mathbf{D}$ is symmetrical ($\mathbf{D} = \mathbf{D}^{\mathrm{T}}$).

The relation between stress and strain may also be stated in the form of strain as a linear function of stress, see Equation 2.4. Where $\mathbf{C}$ is the compliance matrix.

$$\boldsymbol{\varepsilon} = \mathbf{C}\boldsymbol{\sigma} \tag{2.4}$$

By investigating the concept of energy development from strain in the general case, with the assumption that the strain energy is positive when the strain is not equal to zero it has been shown that the constitutive matrix is positive definite, which yield that it may be inverted according to Equation 2.5. For further information regarding strain energy and the constitutive matrix see Ottosen and Petersson (1992).

$$\mathbf{C} = \mathbf{D}^{-1} \tag{2.5}$$

Both the compliance formulation and the generalized form of Hooke's law are equally valid, which one used is in general decided by the circumstances of the problem at hand.

2.2.2   Engineering elastic parameters

Stiffness parameters are traditionally specified by engineering elastic parameters, and not by the compliance or the generalized form of Hooke's law (Bodig and Jayne, 1982). The characteristics of an orthotropic material are specified by six stiffness parameters; three moduli of elasticity (E_1, E_2 and E_3); and three moduli of rigidity or shear moduli (G_{12}, G_{13} and G_{23}). The shear moduli, describe the relations between stress and strain in the same manner as the moduli of elasticity. Forces in one specific direction may cause deformations in lateral directions. The ratio between strain in the loading direction and the lateral direction is termed Poisson's ratio (ν), and is defined with strains in Equation 2.6 and for the compliance form in Equation 2.7. Depending on the symmetry features of a material, different numbers of Poisson's ratio are needed to describe the characteristics. An orthotropic material is characterized by three ratios; ν_{12}; ν_{13}; and ν_{23}.

$$-\nu_{ij} = \frac{\varepsilon_j}{\varepsilon_i} \tag{2.6}$$

$$-\nu_{12} = \frac{C_{21}}{C_{11}} \tag{2.7}$$

All six stiffness parameters are directly connected to the compliance form through Equations 2.2 and 2.4. When the Poisson's ratios are considered all compliance coefficients may be expressed with engineering parameters, according to:

$$
\begin{bmatrix} \varepsilon_1 \\ \varepsilon_2 \\ \varepsilon_3 \\ \varepsilon_{12} \\ \varepsilon_{13} \\ \varepsilon_{23} \end{bmatrix}
=
\begin{bmatrix}
\frac{1}{E_1} & \frac{-\nu_{12}}{E_2} & \frac{-\nu_{13}}{E_3} & 0 & 0 & 0 \\
\frac{-\nu_{12}}{E_1} & \frac{1}{E_2} & \frac{-\nu_{23}}{E_3} & 0 & 0 & 0 \\
\frac{-\nu_{13}}{E_1} & \frac{-\nu_{23}}{E_2} & \frac{1}{E_3} & 0 & 0 & 0 \\
0 & 0 & 0 & \frac{1}{G_{12}} & 0 & 0 \\
0 & 0 & 0 & 0 & \frac{1}{G_{13}} & 0 \\
0 & 0 & 0 & 0 & 0 & \frac{1}{G_{23}}
\end{bmatrix}
\begin{bmatrix} \sigma_1 \\ \sigma_2 \\ \sigma_3 \\ \sigma_{12} \\ \sigma_{13} \\ \sigma_{23} \end{bmatrix}
\tag{2.8}
$$

2.3   Cross-laminated timber

Cross-laminated timber (CLT) panels are structural elements assembled of multiple stacked layers of laminations, where every second layer of laminations are oriented in a 90-degree angle with respect to adjacent layers (Borgström and Fröbel, 2017). The transverse layup of a CLT panel with five layers is shown in Figure 2.3. CLT panels are most often used as floor or wall elements. Wooden components are in general an environment-friendly material, in the manner of being reusable and at the end of its life cycle being used as fuel. Another, environmental benefit is that wood is a lightweight material which reduces the cost of transportation, assembly on the construction site and creating a supporting foundation for the main structure. The possibility to prefabricate CLT elements with the appropriate dimensions, including openings for windows and doors, further reduces the work on the construction site.
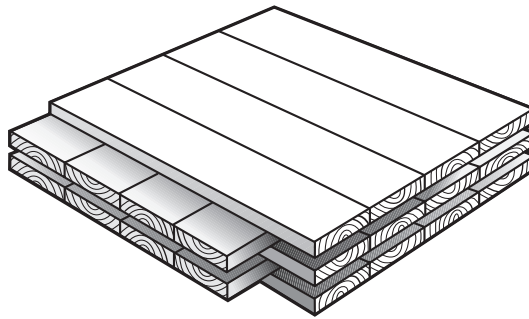
Figure 2.3: An example of a CLT panel built up of five layers of laminations.

The production of CLT in Europe started in the late 1990s and has grown to produce approximately 600 000 m^3 in the year 2018 (Borgström and Fröbel, 2017). In Sweden, CLT was introduced in the end of the 1990s, after the ban of constructing wooden buildings over two stories was lifted in the year 1994, and reached a production around 15 000 m^3 in the year 2014.

2.3.1   Manufacturing

CLT panels are constructed of multiple wooden boards (Borgström and Fröbel, 2017). If the boards are not of sufficient length, they are extended through glued finger joints to achieve the final length of the complete panel. The boards are then planed and an adhesive is applied to both of the wide sides of the boards. Multiple boards are then glued together during constant pressure, either by vacuum or hydraulic pressure to produce the correct dimensions. Lastly, openings for windows and installations, and polishing of visual areas are made before the panels are sent to the construction site.

The dimensions of CLT elements are often restricted by the capacity of the manufacturer and the transportation vehicle (Borgström and Fröbel, 2017). CLT elements may be constructed in a variety of dimensions; the width of CLT panels that occur are between 1.2 – 4.8 m; the thickness varies between 60 – 500 m; and the length are usually up to around 16 m, but lengths up to 30 m are possible. The dimensions of the laminations varies in width between 40 – 300 mm and the thickness between
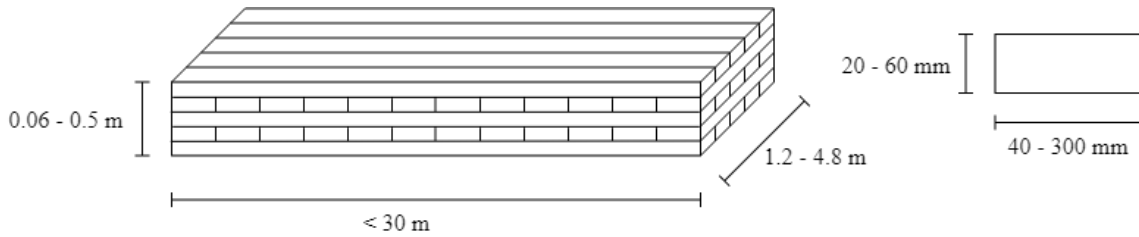
20 – 60 m. All dimensions are shown in Figure 2.4.

Figure 2.4: An example of a CLT element with typical dimensions to the left and typical dimensions of the cross-section of the laminations used for CLT elemenet to the right.

The majority of the stiffness of the CLT panel is received through the plies oriented in the main span direction, but the presence of the transverse layers contributes and these layers are in need of consideration when deflection and stress evaluations are performed (Borgström and Fröbel, 2017). The transverse layers may be subjected to so-called rolling shear depending on the load situation (Aicher and Dill-Langer, 2000). Shear stresses give rise to shear strains perpendicular to the grain. If the shear stresses exceeds the capacity of the wood, shear rolling fractures will occur, which means that the tree fibres separate. The rolling shear stiffness of a timber board is dependent on the pattern of annual rings in the cross-section (sawing pattern). Aicher and Dill-Langer (2000) showed that for different patterns, the rolling shear modulus varies between about 45 – 200 MPa. The largest and the smallest values are although results of sawing patterns where the natural curvature of the annual rings are neglected; vertical; horizontal; with a 45-degree angle. The ratio between the rolling shear modulus and the longitudinal shear modulus of softwood have been showed to be around 1/10 by Fellmoser and Blass (2004). Widely recommended is to use a rolling shear modulus to 50 MPa for multi-layered panels, independent of the softwood species (Aicher and Dill-Langer, 2000).

2.3.2   Gamma-method

Structural timber elements that are mechanically assembled of multiple components, for example, an I-beam, will act less stiff in comparison to a solid element due to the compliance of the connection between the different components (EN 1995-1-1, 2004). A method to handle this effect for elements exposed to bending is reduce the bending stiffness, through the so-called Gamma-method, which is given in EN 1995-1-1 (2004). The reduction method is initially designed for elements consisting of one or multiple sets of flanges and webs, jointed by mechanical connections, but has also been proven applicable for CLT elements (Borgström and Fröbel, 2017).

The theory is applicable to CLT elements with three, five or more layers of laminations (Borgström and Fröbel, 2017). An assumption made when using the Gamma-method is that the layers with laminations where the grain direction of the wood is perpendicular to the direction of interest, only contribute to the bending stiffness through the gamma-factors (γ_i), which are reduction factors. The gamma-factors are affected

by the reference length (l_{ref}) of the CLT panel. The reference length depends on the span length (l) and the β-factor which is dependent on the support condition. Other, affecting parameters are the thickness of the laminations (t_i), the parallel to grain stiffness of the boards oriented with the grain direction in the span direction ($E_{x,i}$) and the rolling shear stiffness ($G_{9090,i}$). Index i represents a layer of the CLT element where the numbering starts from the bottom, see Figure 2.5.
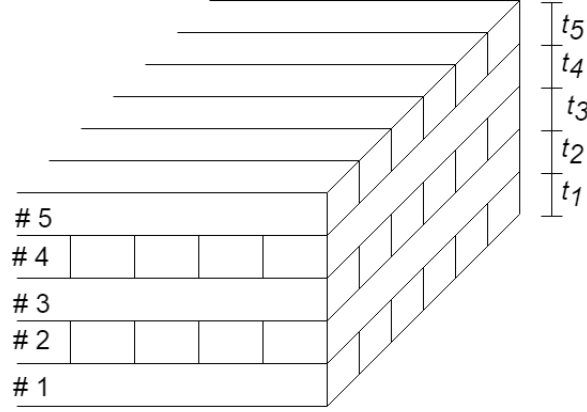
Figure 2.5: Numbering and thickness of layers in a CLT floor slab.

The gamma-factors for a five layered element are calculated as follows:

$$\gamma_1 = \frac{1}{1 + \dfrac{\pi^2 E_{x,1} t_1}{l_{ref}^2} \dfrac{t_2}{G_{9090,2}}} \tag{2.9}$$

$$\gamma_3 = 1 \tag{2.10}$$

$$\gamma_5 = \frac{1}{1 + \dfrac{\pi^2 E_{x,5} t_5}{l_{ref}^2} \dfrac{t_4}{G_{9090,4}}} \tag{2.11}$$

The effective second moment of inertia is then calculated according to Steiner's theorem, where only the layers with laminations where the grain direction of the wood is parallel to the direction of interest are included and with addition of the gamma-factor to the second term:

$$I_{ef} = \sum_{i=1}^{n} \frac{bt_i^3}{12} + \gamma bt_i z^2 \tag{2.12}$$

3 Structural dynamics

This chapter includes the dynamic theory employed to analyse the floor models. The discrete method is first described. Then, an equation to calculate the natural frequency is derived for a beam model seen as a continuous media.

3.1 Introduction

Structures are primary designed according to statical load situations and the dimensions of the structure are often directly related to the magnitude of the resulting force; the greater the force, the larger the dimensions. Dynamic loading, which varies over time may affect structures differently. The impact from time-dependent loads are also affected by the magnitude of the force but the frequency in which the load is varying is also of importance for the structural response. If the excitation frequency of the load corresponds to the frequency were the structure starts oscillating (natural frequency), the response can be significantly amplified.

Vibrations may be described as oscillations around the statical equilibrium of a structure (Chopra, 2012). Vibrations arise when time-varying disturbances, either forces or displacements, interact with the inertia properties of an affected medium (ISO 10137, 2007). When a building is examined for vibration response the characteristics of the vibration source, the transmission path and the receiver must be taken into account (Persson, 2016). The vibration source produces the dynamic forces or displacements, and are in general a function of time and space. The transmission path is the medium in which the vibrations from the source is propagated to the receiver, the vibrations are affected by the properties of the medium. The receiver is the object where the resulting vibrations are assessed and evaluated with the applicable criteria of the specified serviceability limit state. The receiver can be a component of a building structure, contents of the building (instruments, machines etc.) or human occupants.

The dynamic response of a structural system is affected by the material properties, the properties of the system as whole, and the presence of non-structural elements, such as floor coverings, ceilings etc. (ISO 10137, 2007). Discontinuities and attenuations due to imperfections within the material have an effect as well as connections between different structural elements. All structural and non-structural elements contribute to the inertia, elastic and energy dissipation properties of the structure (Chopra, 2012). When idealizing a system these properties are divided into separate components with one of the properties; mass (inertia); stiffness (elastic); and damping (energy dissipation).

3.2 Equation of motion

Modelling a structure may be complicated, normally simplifications are made to discretise the system. The structural elements are divided into nodes with one or multiple degrees of freedom (DOF), which are able to represent the displacements to describe any possible deformation of a structure (Chopra, 2012). A DOF may represent either a displacement or a rotation. The required number of DOFs vary between different systems, to describe any possible position at any given time. Depending on the components of a structural system different simplifications may be performed to idealize the system. It is of importance that the model can represent the behaviour of the original system.

3.2.1 Single-degree-of-freedom system

The easiest way to model a structure is with a single-degree-of-freedom (SDOF) system (Chopra, 2012). The system is consisting of a body with lumped mass, a spring and a damper, representing the stiffness and damping, respectively. The spring and the damper are considered massless. The only allowed motion is in the horizontal direction, in which a dynamic force ($p(t)$) is applied. The reaction forces from the spring (f_s) and the damper (f_c) are acting in the opposite direction of the applied force. The displacement (u), velocity ($\dot{u}$) and acceleration ($\ddot{u}$) are defined positive in the direction of the force. To derive the equation of motion the system is translated into a free body diagram. The system and the free body diagram are shown in Figure 3.1.
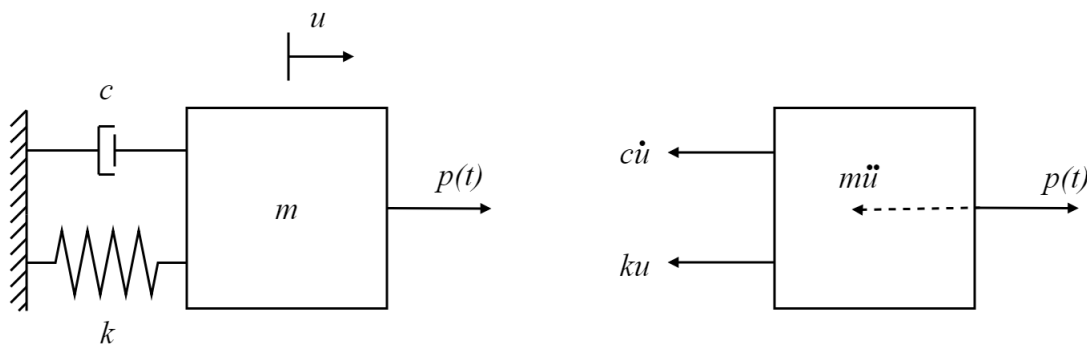
Figure 3.1: The SDOF system is displayed to the left; translated into a free body diagram shown to the right.

When a linear system is considered the relation between the resulting spring force (f_s) and the deformation (u) is linear (Chopra, 2012). The same linear relation applies for the damper force (f_c) to the velocity ($\dot{u}$). This results in the two following equations:

$$f_s = ku \tag{3.1}$$

$$f_c = c\dot{u} \tag{3.2}$$

To derive the equation of motion, Newton's second law of motion is implemented and the previous equations defining the spring and damper forces are used.

$$p(t) - f_s - f_c = m\ddot{u} \tag{3.3}$$

$$m\ddot{u} + c\dot{u} + ku = p(t) \tag{3.4}$$

The displacements are received by solving the equation, from which internal forces and moments may be calculated.

3.2.2 Multi-degree-of-freedom system

As earlier stated, in most of the cases when idealizing a structure through a discrete model, multi-degree-of-freedom (MDOF) system is needed to describe the behaviour of the structure. A finite number of nodes with a finite number of DOFs are defined (Chopra, 2012). The system is assumed to be fully linear (all non-linear behaviour is neglected) and with Newton's second law of motion, Equations 3.1 and 3.2 describing the spring and damper relation the equation system of the structural system is expressed. The result is an extended formulation of the SDOF equation of motion:

$$\mathbf{M}\ddot{\mathbf{u}} + \mathbf{C}\dot{\mathbf{u}} + \mathbf{K}\mathbf{u} = \mathbf{p}(t) \tag{3.5}$$

where $\mathbf{M}$ represent the mass matrix, $\mathbf{C}$ the damping matrix and $\mathbf{K}$ the stiffness matrix. The displacements ($\mathbf{u}$), velocities ($\dot{\mathbf{u}}$), accelerations ($\ddot{\mathbf{u}}$) and the excitation force ($\mathbf{p}(t)$) are represented by vectors. For a finite system with n DOFs, the matrices are of size $n \times n$ and the vectors of size $n \times 1$. The equation may be solved analytical or numerical, which method that is applicable is dependent on the complexity of the system and equation.

3.3 Eigenfrequencies and modes of vibration

All structural systems have an infinite number of natural frequencies, in which the structure vibrates around its statical equilibrium (Chopra, 2012). Each natural frequency has its own particular pattern of deformation, which can be expressed with modal coordinates (q_n). Together, the modal coordinates describe the shape of a particular natural frequency, the natural mode (ϕ_n). Analysing natural frequencies and modes are performed with a system subjected to free vibration. Free vibration may be defined as a structure in motion which is not subjected to any dynamic excitation. The motion can be initiated by applying disturbances to the structure, either by adding some initial deformation to the original static equilibrium or by applying initial velocity or in a combination of both. The system subjected to free vibration by an initial deformation according to a natural mode will vibrate in simple harmonic motion, the displacement of each node will reach their maximum and minimum simultaneously and maintain the initial deflected shape. Figure 3.2 shows the displacement of a node in free vibration.

The time required for a system to go through one full harmonic motion of the natural mode is called the natural period of vibration (T_n). The natural cyclic frequency of
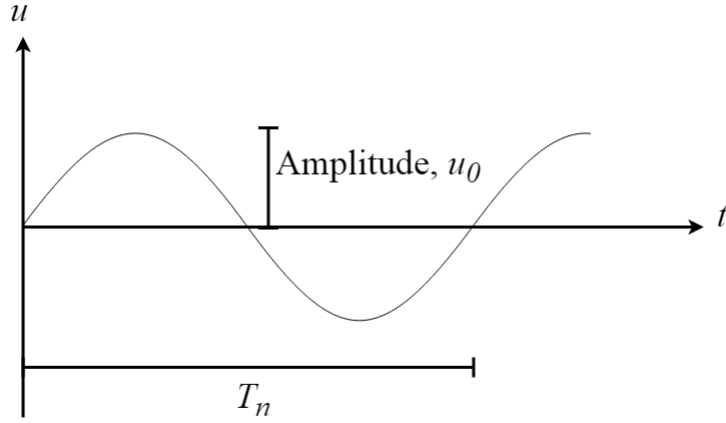
Figure 3.2: The displacement of a node in relation to time. The amplitude of the node and the natural period of vibration is shown.

vibration (natural frequency, f_n) and the corresponding natural circular frequency of vibration (angular natural frequency, ω_n) and their relationship are shown in Equations 3.6 and 3.7 below.

$$f_n = \frac{1}{T_n} \tag{3.6}$$

$$\omega_n = 2\pi f_n \tag{3.7}$$

The vibration response is governed by the equation of motion (Equation 3.5) but with the condition that the initial excitation force vector ($\mathbf{p}(t)$) is equal to zero, which results in:

$$\mathbf{M\ddot{u} + C\dot{u} + Ku} = 0 \tag{3.8}$$

An undamped system (damping is neglected) is analysed here after. The damping is an energy dissipating effect, which decays the motion of free vibration and the natural circular frequency (Chopra, 2012). The damping has a negligible effect on the value of a natural frequency. The reduction of the equation of motion will result in:

$$\mathbf{M\ddot{u} + Ku} = 0 \tag{3.9}$$

To solve the equation system with respect to the initial conditions $u(0) = u_0$ and $\dot{u}(0) = \dot{u}_0$, an eigenvalue problem is introduced. The free vibration response of an undamped system in a specific natural frequency and mode can be expressed mathematically by the modal coordinates and the natural mode shape:

$$\mathbf{u}(t) = q_n(t)\phi_n \tag{3.10}$$

16

The mode shape is assumed to be constant and the time dependency is handled by describing the modal coordinates with a simple harmonic function:

$$q_n(t) = A_n \cos(\omega_n t) + B_n \sin(\omega_n t) \tag{3.11}$$

The initial conditions can be used to determine the constants A_n and B_n. Equations 3.10 and 3.11 combined gives Equation 3.12, where ω_n and ϕ_n are unknown.

$$\mathbf{u}(t) = \phi_n(A_n \cos(\omega_n t) + B_n \sin(\omega_n t)) \tag{3.12}$$

By substitution with Equations 3.11 and 3.12 to Equation 3.9, and by reducing the system with the fact that if $q_n(t)$ is equal to zero implies that there is no motion to the system ($\mathbf{u}(t) = \mathbf{0}$). A system with no motion is called the trivial solution and are not of interest here. These conditions give:

$$[\mathbf{K} - \omega_n^2 \mathbf{M}]\phi_n = \mathbf{0} \tag{3.13}$$

This algebraic equation is called the matrix eigenvalue problem (Chopra, 2012). $\mathbf{K}$ and $\mathbf{M}$ are known; ω_n and ϕ_n are required to satisfy the equation. The equation system may be seen as a number of equations equal to the number of nodes within the structural model and each equation representing one of the nodes. $\phi_n = \mathbf{0}$ is another trivial solution which is not of interest and implies no motion. The equation has a non-trivial solution if Equation 3.14 is satisfied, which is known as the characteristic equation or the frequency equation (Chopra, 2012).

$$det[\mathbf{K} - \omega_n^2 \mathbf{M}] = \mathbf{0} \tag{3.14}$$

The solution to the characteristic equation will result in a polynomial answer of the same order as the number of elements analysed in the system (Chopra, 2012). The answer will be real and positive roots for ω_n^2 which describes the eigenfrequencies of the system. The corresponding mode shapes to the eigenfrequencies may be calculated with Equation 3.13, which describes the shape through the positions of the different nodes, and not the amplitude of the oscillating behaviour.

3.4   Vertical vibration continuous media

A structural element in a dynamic excitation may also be analysed as a continuous media, instead of using the discrete method through a finite element analysis, earlier explained in this chapter. A continuous media analysed in dynamic response requires the derivation of the equation of motion for a differential volume element (Bodig and Jayne, 1982). Instead of lumping the material properties they are distributed along the element, which results in that the analysis takes a more realistic approach but the

complexity increases remarkably. Some assumptions made when analysing a continuous media is that the cross-section is small in relation to the length of the element which results in that the wavelength of the vibration is large in relation to the cross-sectional dimensions, the section plane remains plane throughout the vibration, the material is assumed to be continuous in cross-section and the material is homogeneous.

A beam representing a floor in one dimension will be analysed for flexural vibrations to derive the equation to determine the natural frequencies. In Figure 3.3 the beam is shown subjected to oscillations perpendicular to the length of the element and a small part of the element with a length of dx is shown with the resulting shear forces (F) and bending moment (M), both the shear and moment vary along the length.
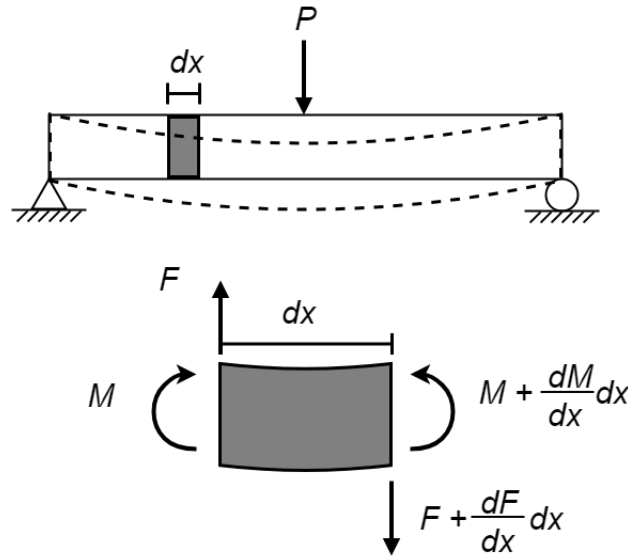
Figure 3.3: The beam model analysed for flexural vibrations to derive the equation to determine the natural frequencies.

To derive the equation to calculate the fundamental frequency of the beam, a force equilibrium and a moment equilibrium of the beam part are performed. Introducing Newton's second law of motion and by describing the moment as the product of the second derivative of displacement and the bending stiffness of the beam, the following equation may be formulated:

$$\frac{d^2 u}{dt^2} = \frac{EI}{\rho A} \frac{d^4 u}{dx^4} \tag{3.15}$$

The general solution may be described with either an exponential or by a hyperbolic function due to the mathematical relation and with the prescribed condition that all constants may be determined and a solution may be obtained (Bodig and Jayne, 1982). The exponential solution is chosen to be used:

$$u = C_1 e^{\alpha x} + C_2 e^{\alpha x} + C_3 \cos \alpha x + C_4 \sin \alpha x \tag{3.16}$$

The trial solution should be chosen as a function for which the fourth derivative is the same function as itself. An exponential function with two constants (u_0 and a) which

fulfils this condition is chosen.

$$u = u_0 e^{ax} \tag{3.17}$$

Due to the dynamic evaluation of the element and that the motion of the element will be periodical in the vibration, it is assumed that the displacement can be described by the function:

$$u = u_0 \cos(\omega t - \varphi) \tag{3.18}$$

The displacement (u) on the left-hand side is a function of time and the right-hand side is a function of position, which implies that both must be constants and therefore the acceleration must be constant (Bodig and Jayne, 1982). By selecting the location of maximum displacement the cosine term of the equation may be reduced. By substitution of the forth derivative of Equation 3.17 and the reduced form of Equation 3.18, into Equation 3.15 gives:

$$a^4 e^{\alpha x} = -\omega^2 \frac{\rho A}{EI} \tag{3.19}$$

For x = 0 the equation has four different solutions where a is equal to $\pm \alpha$ and $\pm i\alpha$, where:

$$\alpha = \left| \omega^2 \frac{\rho A}{EI} \right|^{1/4} \tag{3.20}$$

α describes the wavelength of a sinusoidal wave in relation to the position, x. A complete cycle is defined as 2π, which correspond to the natural period of vibration (T_n), $x = T_n$, see Figure 3.2. Therefore, $\alpha = 2\pi/T$ for a complete cycle. Squaring both sides of Equation 3.20 and rearrange the parameters gives:

$$\omega = \left(\frac{2\pi}{T_n} \right)^2 \sqrt{\frac{EI}{\rho A}} \tag{3.21}$$

At resonance, the beam oscillates with a infinite number of waves. Both ends of the beam are prescribed for displacements but in between the beam move freely (Bodig and Jayne, 1982). At the first mode of vibration, the wavelength is twice as long as the element, for the second it is the same length as the element. The general relation between the length of the element and the wavelength are defined as $T = 2l/n$, where n represent the order of the natural frequency. The relation between the angular natural frequency and the natural frequency are shown in Equation 3.7, substitution with these two equations leads to an expression to calculate the natural frequencies for a freely supported beam:

$$f_n = \frac{\pi n}{2l^2} \sqrt{\frac{EI}{\rho A}} \tag{3.22}$$

The equation to calculate the fundamental frequency, the first natural frequency, where $n = 1$, becomes:

$$f_1 = \frac{\pi}{2l^2} \sqrt{\frac{EI}{\rho A}} \qquad (3.23)$$

3.5 Damping

Damping is in practice very complicated to determine for a finite element analysis of a structural system because of the multiple different features that are contributing to the energy dissipating effect (Chopra, 2012). As earlier stated, the damping is affected by material parameters as well as structural components and configurations. In addition to this, the damping properties are dependent on the frequency which further complicates the issue. Damping can be handled by specifying modal damping ratios, which are numerical values based on results from experimental tests (Bathe, 2016). The damping matrix is necessary to include for some analysis and can be constructed using the stiffness and mass matrices of the complete element assemblage. Different methods of constructing damping matrices are given in Bathe (2016).

In this Master's dissertation, the damping is neglected due to the negligible effect on the eigenfrequencies. The system is considered as a system of low damping which implies that the damping matrix may be neglected. Moreover, the recommended design criteria of the fundamental frequency supplied by EN 1995-1-1 (2004), (see Chapter 4) does not include any compensation for damping, which the results of the eigenfrequency analysis will compare with in Chapter 5.

4 Design methods and recommendations

Recommended design methods regarding vibrations available in literature are presented in this chapter. Recommended material properties of structural timber is presented. Finally, an evaluation of the CLT floor which later is analysed with the FE method in Chapter 5 is performed according to the recommended criteria of the first natural frequency.

4.1 International Organization for Standardization

The International Organization for Standardization (ISO) is a global federation of national standard bodies (ISO 10137, 2007). ISO consists of member bodies, which form technical committees to work on preparing international standards regarding various subjects of interest. International organizations, governmental and non-governmental may also take part in the work. 75 percent of the member bodies must approve a publication before it will be published as an international standard.

Serviceability of buildings, which include regulations regarding vibrations in building components, are mainly considered in ISO 10137 (2007). The vibration criteria in the serviceability limit state for buildings is based on the receiver. A receiver may be different objects depending on the circumstances; building contents; building structures; and human occupants (ISO 10137, 2007).

Buildings may include sensitive instruments or manufacturing processes and the vibration criteria should in such cases assure satisfactory functionality. The serviceability criteria for building structures concern minor or visual damage to elements, for example, visual cracks in concrete. The allowed level of damage depends on the type of structure, age, importance, state of repair etc.

The human level of acceptance to vibrations are dependent on multiple factors. In general, the acceptance is very individual and it is affected by the environment of which the vibrations are experienced in. Most often when the human response to vibrations is analysed the frequency range 1 to 80 Hz is considered, 0.063 to 1 Hz may also be considered during some circumstances. The assessment of probable human response to vibrations is further given in ISO 10137 (2007).

4.2 Eurocode

The Eurocodes are a series of European standards developed by the European Committee for Standardization (CEN) to provide design approaches for construction work and structural design. The expectation was to harmonise the technical rules of construction and contribute to a uniform level of safety within the European Union (European Commission, 2019). Eurocode includes design recommendations regarding the basis of structural design, design of different construction materials, actions on structures, structural fire design, geotechnical design and hazard design as earthquake. Eurocode 5 deal with design of timber structures and includes design recommendations regarding floor vibrations, which further will be used in this dissertation (EN 1995-1-1, 2004).

4.2.1 Design criterion for vibrations

The design criteria for vibrations of structural components are divided into three sections in Eurocode 5: General; Vibrations from machinery; and Residential floors (EN 1995-1-1, 2004). Mainly, the third section is of interest when evaluating floor elements but the first section includes some guidelines that affect floor elements. The component or structure shall be ensured to not cause vibrations that can impair the function of the structure or cause unacceptable discomfort to the users from reasonably anticipated actions. The vibration level should further be evaluated by measurements or by calculations with regards to the structural stiffness and the modal damping ratio. The modal damping ratio (ζ) should be equal to 1 %, if not other values are proven more accurate.

The vibration analysis for residential floors in Eurocode 5 is applicable to floors with a fundamental frequency greater than 8 Hz ($f_1 > 8$ Hz). If the frequency is lower than 8 Hz, a detailed investigation should be performed (EN 1995-1-1, 2004). For residential floors with a fundamental frequency greater than 8 Hz, the following requirements should be satisfied:

$$\frac{w}{P} \leq a \text{ [mm/kN]} \tag{4.1}$$

and

$$v \leq b^{(f_1\zeta-1)} \text{ [m/(Ns}^2)]} \tag{4.2}$$

where w is the maximum instantaneous vertical deflection caused by a vertical concentrated static force P applied at any point on the floor, taking account of load distribution, v is the impulse velocity response (see Equation 4.4) and ζ is the modal damping ratio. a and b are values for control of the stiffness and the impulse response, respectively. The recommended range for a and b and their relation is shown in Figure 4.1. Information on the national choice may be found in the National annex, for Swedish standards the values have been set to $a = 1.5$ mm/kN and $b = 100$ m/(Ns^2) by Boverket (2016). The fundamental frequency for a rectangular floor, simply supported
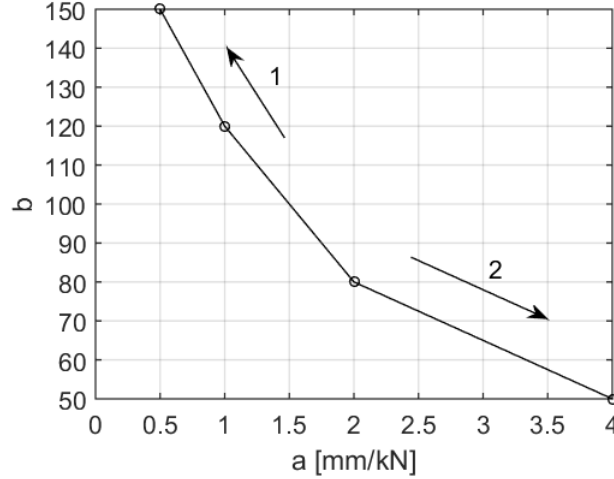
Figure 4.1: The recommended range and relation between a and b according to Eurocode 5. Direction 1 result in higher performance and direction 2 in poorer performance (EN 1995-1-1, 2004)

along two opposite sides and unsupported on the other two sides may be calculated according to Equation 4.3, which is derived in Section 3.4, while, the impulse velocity response for a floor may according to EN 1995-1-1 (2004) be calculated according to Equation 4.4. The mass (m) only considers the self weight of the floor and is expressed in mass per metre, l represents the span length between the supports in metres, b the width of the floor perpendicular to the span direction and $(EI)_l$ is the equivalent bending stiffness of the floor in the span direction.

$$f_1 = \frac{\pi}{2l^2} \sqrt{\frac{(EI)_l}{m}} \tag{4.3}$$

$$v = \frac{4(0.4 + 0.6n_{40})}{mbl + 200} \tag{4.4}$$

n_{40} is the number of first-order modes with natural frequencies up to 40 Hz. The value of the first-order modes with natural frequencies up to 40 Hz may be calculated with Equation 4.5. The equivalent plate bending stiffness perpendicular to the main direction $((EI)_b)$ is considered, which should be less than the bending stiffness in the span direction $((EI)_b < (EI)_l)$.

$$n_{40} = \left\{ \left(\left(\frac{40}{f_1}\right)^2 - 1 \right) \left(\frac{b}{l}\right)^4 \frac{(EI)_l}{(EI)_b} \right\}^{0.25} \tag{4.5}$$

4.2.2 Strength classes of wood

To ensure a certain level of continuity of the selection of material parameters and minimize a large verity of results when designing wooden components from an engineering perspective, the CEN has published standards containing material strength classes and their material parameters (EN 338, 2016). Strength classes of wood are

published in EN 338 (2016). To further ensure a constant level of safety of designed structures and due to the large verity of the wooden features, the characteristic value is chosen as the fifth percentile of the strength or stiffness distribution. Tension and bending tests are commonly performed to identify properties of wood-based structural elements. For softwoods (which are most commonly used in Sweden), the resulting strength classes determined from tension tests are named Txx, the strength classes determined form bending tests are named Cxx, where xx refers to the fifth percentile of which strength test that has been performed. The most common strength classes and corresponding properties are shown in Table 4.1. Hardwood spices tested in bending are named Dxx. For some kinds of hardwood which have features similar to softwood the strength classes Txx and Cxx may be used.

Table 4.1: Strength, stiffness and density for the most commonly used strength classes of softwood (EN 338, 2016).

	Class	C16	C24	C30	T11	T14	T22
Strength prperties in N/mm^2							
Bending	$f_{m,k}$	16	24	30	17	20.5	30.5
Tension parallel	$f_{t,0,k}$	8.5	14.5	19	11	14	22
Tension perpendicular	$f_{t,90,k}$	0.4	0.4	0.4	0.4	0.4	0.4
Compression parallel	$f_{c,0,k}$	17	21	24	18	21	26
Compression perpendicular	$f_{c,90,k}$	2.2	2.5	2.7	2.2	2.5	2.7
Shear	$f_{v,k}$	3.2	4.0	4.0	3.4	4.0	4.0
Stiffness properties in kN/mm^2							
Mean modulus of elasticity parallel bending/tension	$E_{0,mean}$	8.0	11.0	12.0	9.0	11.0	13.0
5 percentile modulus of elasticity parallel bending/tension	$E_{0,k}$	5.4	7.4	8.0	6.0	7.4	8.7
Mean modulus of elasticity perpendicular	$E_{90,mean}$	0.27	0.37	0.40	0.30	0.37	0.43
Mean shear modulus	G_{mean}	0.5	0.69	0.75	0.59	0.69	0.81
Density in kg/m^3							
5 percentile density	ρ_k	310	350	380	320	350	390
Mean density	ρ_{mean}	370	420	460	380	420	470

4.3 Analytic evaluation of wooden floor slab

CLT panels are typically manufactured with three to seven layers of laminations. In this dissertation, a floor slab with five equally thick layers is chosen to be analysed. The dimensions of the floor are set to be 6 m × 3 m, with a total height of 200 mm. All laminations are of the dimension 150 mm × 40 mm. The floor and all dimensions are shown in Figure 4.2.
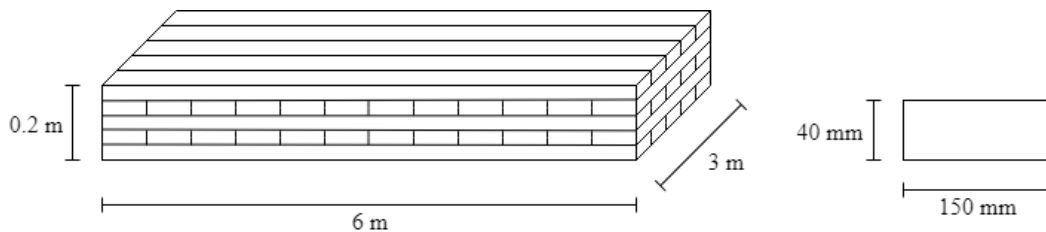
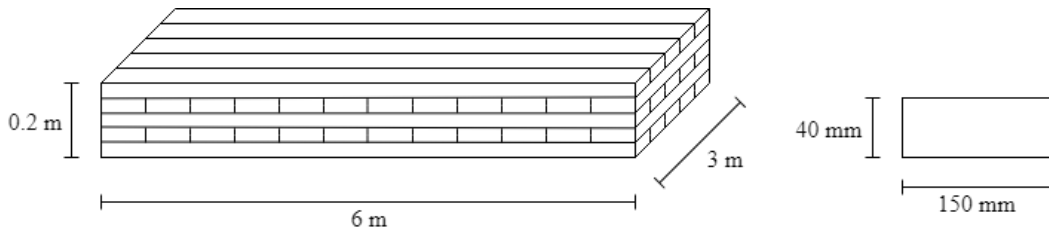**Figure 4.2:** The dimensions of the CLT floor slab (to the left) and the dimensions of the individual laminations (to the right).

The floor is simply supported along the to sides that are 3 m. The strength class chosen for all individual laminations is C24 according to EN 338 (2016), which is one of the most commonly used in Sweden. All the stiffness properties and the density (ρ) can be found in EN 338 (2016), with the exception of the rolling shear stiffness which is taken from Borgström and Fröbel (2017). The material parameters are presented in Table 4.2

Table 4.2: The stiffness parameters and the density used during the analytic evaluation. All stiffness parameters are expressed in MPa and the density in kg/m^3.

E_1	E_2	G_{12}	G_{23}	ρ
11 000	370	690	50	420

CLT floor slabs may be designed for vibration resistance in serviceability limit state according to Eurocode 5. Earlier stated in Section 2.3.1, the bending stiffness of a CLT element is greatly affected by the rolling shear stiffness of the laminations. The suggested design procedure according to Borgström and Fröbel (2017) is to apply the Gamma-method according to Section 2.3.2.

4.3.1 Effective second moment of inertia

When calculating the effective second moment of inertia of a CLT floor, the assumption is made that the layers of laminations that have their grain direction perpendicular to the main span direction only contributes to the bending stiffness in the calculations of the gamma-factors. The layers that have their grain direction in the same orientation as the main span contributes to the bending stiffness through the gamma-factors as well as their individual second moment of inertia (Borgström and Fröbel, 2017). For the CLT floor slab analysed the first, third and fifth layers are therefore considered to contribute with their individual second moment of inertia and the calculation of the gamma factors, while the second and fourth layer only contributes to the gamma-factors, according to Figure 4.3.
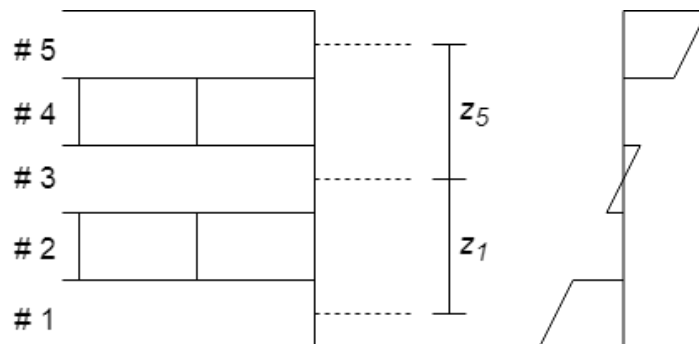
Figure 4.3: The layers contributing to stiffness for the calculation of the effective second moment of inertia. Conceptional normal stress distribution in the effective layers at bending are displayed and the individual lever arms (z_i) between the neutral layer of the floor and the individual layers of laminations are indicated.

The reduction factors (γ_1, γ_3 and γ_5) are calculated according to Equations 2.9 – 2.11. The reference length (l_{ref}) is 6 m, all lamination thickness (t_i) are 40 mm, the stiffness in the span direction of the three layers considered are 11 000 MPa and the rolling shear stiffness is 50 MPa. The calculated reduction factors are shown in Table 4.3.

Table 4.3: The resulting reduction factors for the CLT floor, calculated accordingly to Borgström and Fröbel (2017).

Reduction factor	
Layer 1, γ_1	0.91
Layer 3, γ_3	1
Layer 5, γ_5	0.91

The effective second moment of inertia is then calculated with the reduction of gamma-factors to the second term of Steiner's theorem, according to Equation 2.12. The first, third and fifth layer are considered in the calculation.

$$I_{ef,l} = 0.0014488 \text{ m}^4$$

4.3.2   Fundamental frequency

The fundamental frequency (the first eigenfrequency) is calculated according to Equation 4.3. The mass used is the density multiplied with the total height of the floor (0.2 m) and the width (3 m), which result in a mass of 252 kg/m. The span length is 6 metres. The stiffness in the span length (E_x) is equal to 11 000 MPa and the effective second moment of inertia is 0.0014488 m^4. The fundamental frequency according to Eurocode 5 is:

$$f_1 = 10.973 \text{ Hz}$$

5 Finite element modelling of CLT floor

In this chapter, the created FE models and the results of the analyses are presented. First, an overview of the analysed CLT floor is given, including dimensions and material properties. Four differently advanced models are created; *3D-model with internal laminations*; *3D-model with separate layers*; *2D composite model*; and *2D plate model*. Finally, a summary of the results is given.

5.1 General properties of finite element models

The wooden floor analysed is a CLT floor slab with the dimensions 6 m × 3 m and a height of 200 mm. The floor contains five layers of laminations. All laminations have a cross-section of 150 mm × 40 mm and their length are either 3 m or 6 m, depending on which direction they are oriented in. See Figure 5.1 for all dimensions of the floor and the laminations.

Figure 5.1: The dimensions of the entire CLT floor (to the left) and the dimensions of the individual laminations (to the right).

The strength class of the laminations analysed is chosen as C24, the three Young's moduli (E) and the three shear moduli (G) used can be found in EN 338 (2016), the Poisson's ratio (ν) of spruce are found in Danielsson (2013). All material properties are shown in Table 5.1, where all stiffness parameters are expressed in MPa and Poisson's ratio is unitless. All individual laminations of the floor have the same material properties. The grain direction of every second layer is oriented perpendicular to the direction of the span length. The mass density is also found in EN 338 (2016), for strength class C24, the mean density is 420 kg/m^3.

Table 5.1: The local stiffness parameters, Poisson's ratios and density selected for the laminations are for spruce of strength class C24. All stiffness parameters are expressed in MPa, Poisson's ratio is unitless and the density is expressed in kg/m^3.

E_1	E_2	E_3	ν_{12}	ν_{13}	ν_{23}	G_{12}	G_{13}	G_{23}	ρ
11 000	370	370	0.51	0.38	0.31	690	690	50	420

5.2 Validation of FE models

To be able to validate the simulated eigenfrequencies of the different FE models a comparison must be performed. In this dissertation, the frequencydifference is chosen to be evaluated accordingly:

$$frequencydifference_i = \frac{f_i - f_{ref,i}}{f_{ref,i}} \tag{5.1}$$

where $f_{ref,i}$ is the simulated eigenfrequency of the reference model, which is selected as the model analysed with the finest mesh during the *Mesh convergence studies* and as the *3D-model with internal laminations* when the different FE models are compared to each other, in Section 5.7. f_i is the eigenfrequency which is compared to the reference frequency of a model with a certain mesh size. Notice, that the equation is able to distinguish if the FE models results in higher or lower frequencies than the simulation of the reference. Frequencies that are higher than the reference frequencies will result in a positive value, while a lower frequency will result in a negative value.

5.3 3D-model with internal laminations

The first model assembled is 3D and most correct according to the actual CLT floor design. In Abaqus, the model is created as a solid block with the outer dimensions $6 \times 3 \times 0.2$ m^3. Partitions are used to create the individual laminations and cut to create the gaps of 0.2 mm between all laminations. The FE model created is shown in Figure 5.2.

The stiffness parameters are assigned to the model through *Engineering Constants*, in Abaqus. The material properties that are selected for the model are given in Table 5.2 below:

Table 5.2: Stiffness parameters and Poisson's ratios used. All stiffness parameters are expressed in MPa, Poisson's ratio is unitless and the density is given in kg/m^3.

E_1	E_2	E_3	ν_{12}	ν_{13}	ν_{23}	G_{12}	G_{13}	G_{23}	ρ
11 000	370	370	0.51	0.38	0.31	690	690	50	420
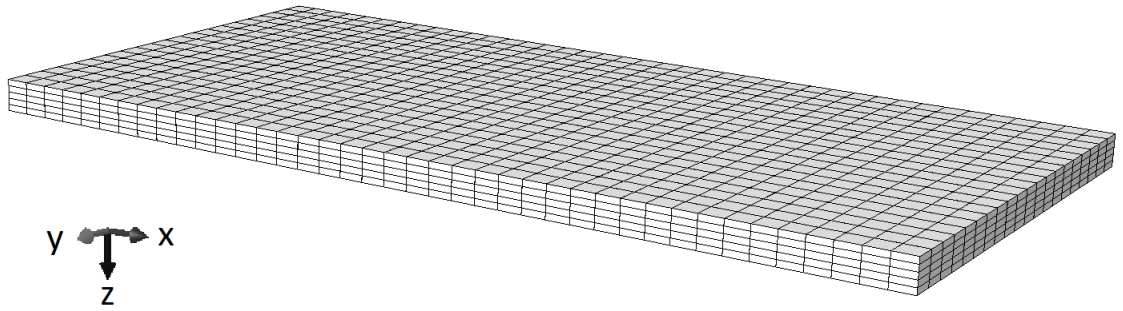
Figure 5.2: The floor modelled as a 3D part consisting of all individual laminations, including a 0.2 millimetres gap between all laminations. The global coordinate system is shown beside the model.

5.3.1 Mesh convergence study

The convergence study is performed in Abaqus with 8-node hexahedral elements using linear approximation and full integration (C3D8 elements). The results of the convergence study of the eigenfrequencies below 80 Hz is shown in Figure 5.3. The thickness of each ply of laminations is divided into two and four layers, respectively, which result in that the entire thickness of the floor is divided into 10 or 20 equal parts. The mesh size in the xy-plane is limited by the fixed width of the laminations, which results in that the element side length evaluated are: 0.15, 0.075 and 0.0375 m. The eigenfrequencies of the model with the finest mesh, 20 layers and 0.0375 m $\times$ 0.0375 m FE elements, is assumed to be most accurate and is chosen as the reference model for the convergence study.

The boundary conditions are applied so the two opposite end-edges of the span length are simply supported while the other two are unsupported. To be able to make a comparison to the floor considered as a one-dimensional beam according to EN 1995-1-1 (2004), the boundary conditions are specified in the centre of the thickness of the floor. The two supported end-edges are prescribed regarding displacements in the global z-direction and one of them is also prescribed in the x-direction. One node on the end corner of each supported edge are prescribed regarding displacements in the y-direction.

5.3.2 Eigenfrequencies and mode shapes

The model with linear elements, where each internal layer is divided into two parts and then four parts, which results in a total of 10 and 20 elements,respectively, in the thickness of the model, was analysed. The first eight eigenfrequencies calculated for the model with the finest mesh size in the xy-plane are shown in Table 5.3.

29

Table 5.3: The eigenfrequencies of the 3D model consisting of all internal laminations. Linear elements are used. The eight first eigenfrequencies are presented for the mesh size of 0.0375×0.0375 m^2 in the xy-plane. The thickness of the floor is divided into 10 and 20 layers, respectively.

No. of Layers	$f_{n,1}$	$f_{n,2}$	$f_{n,3}$	$f_{n,4}$	$f_{n,5}$	$f_{n,6}$	$f_{n,7}$	$f_{n,8}$
10	10.948	15.057	38.733	42.799	53.193	70.345	74.855	78.529
20	10.950	14.968	38.751	42.717	53.194	70.206	74.929	78.506

The corresponding mode shapes using the model with the finest mesh are given in Figure 5.4. The simulated eigenfrequencies are given in the figure caption of each subfigure. The first, thrid and seventh mode shapes corresponds to the first, second and third bending mode, respectively. The second mode shape corresponds to the first torsional mode. The fourth, fifth, sixth and eighth mode shapes includes torsion.
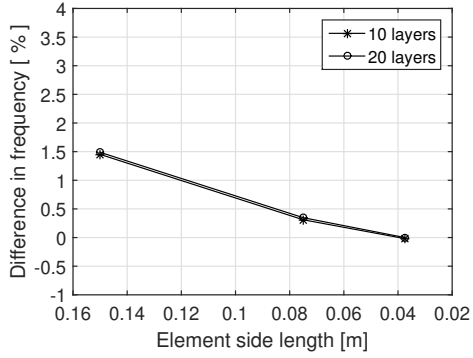
(a) The first eigenfrequency.
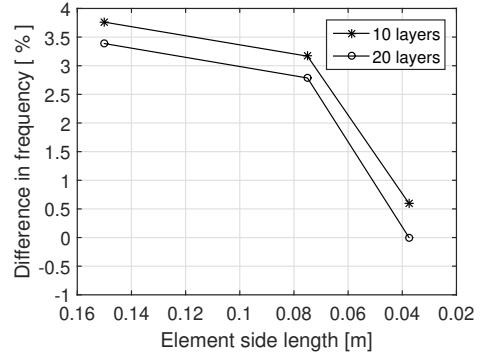
(b) The second eigenfrequency.
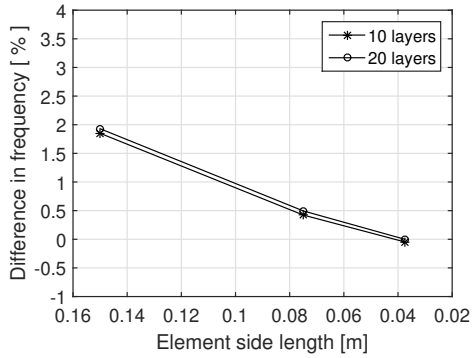
(c) The third eigenfrequency.
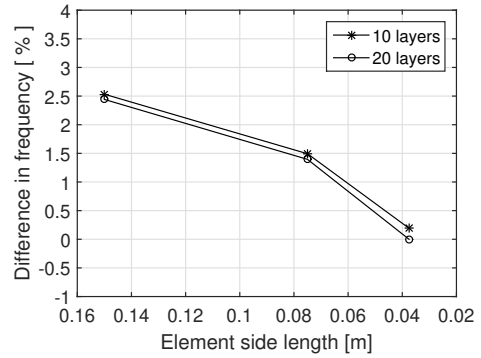
(d) The fourth eigenfrequency.
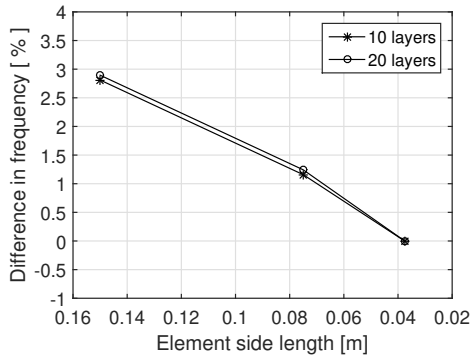
(e) The fifth eigenfrequency.

(f) The sixth eigenfrequency.
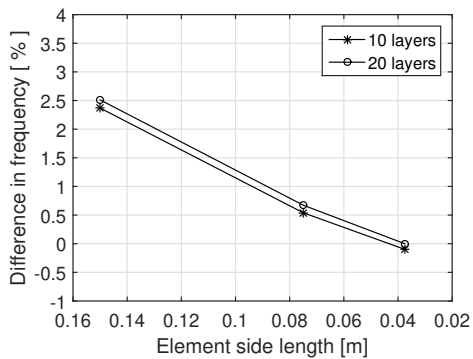
(g) The seventh eigenfrequency.
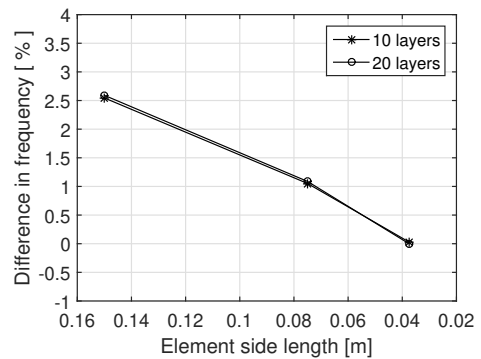
(h) The eighth eigenfrequency.

Figure 5.3: Convergence study of the first eight eigenfrequencies, with linear elements. The study is performed with the thickness of the floor divided into 10 and 20 layers, respectively. The element side length is shown on the horizontal axis. The model with the finest mesh size is selected as reference model. The frequency difference in comparison to the reference frequency is expressed in percent on the vertical axis.
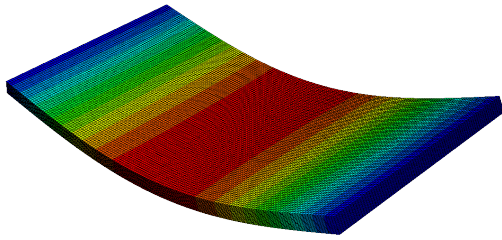
(a) Mode shape of the first eigenfrequency, at the frequency 10.950 Hz.
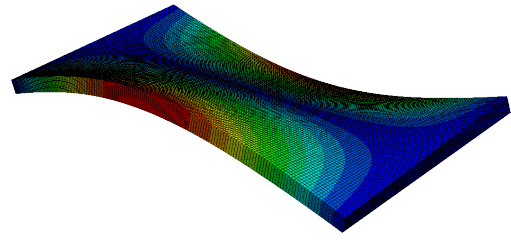
(b) Mode shape of the second eigenfrequency, at the frequency 14.968 Hz.
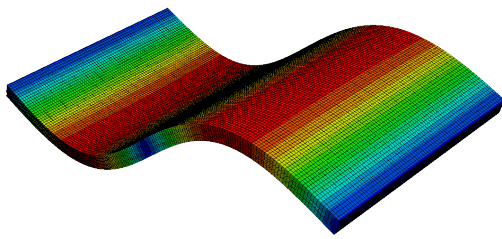
(c) Mode shape of the third eigenfrequency, at the frequency 38.968 Hz.
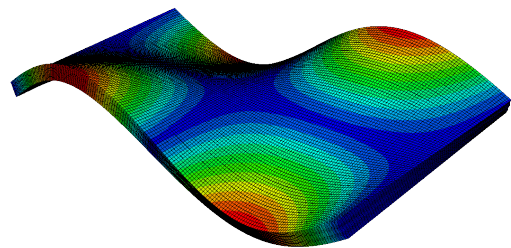
(d) Mode shape of the fourth eigenfrequency, at the frequency 42.717 Hz.
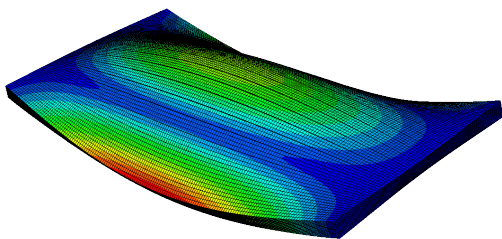
(e) Mode shape of the fifth eigenfrequency, at the frequency 53.194 Hz.
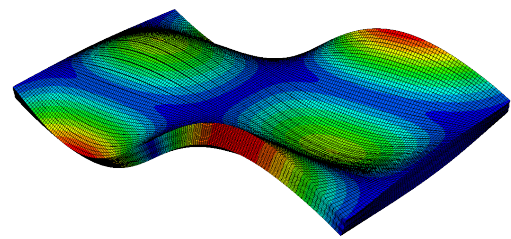
(f) Mode shape of the sixth eigenfrequency, at the frequency 70.206 Hz.
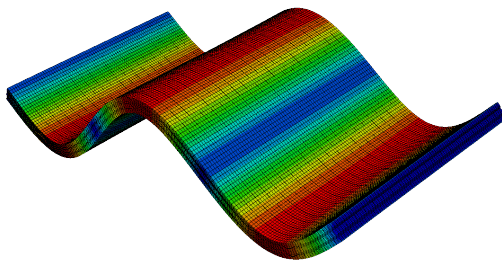
(g) Mode shape of the seventh eigenfrequency, at the frequency 74.929 Hz.
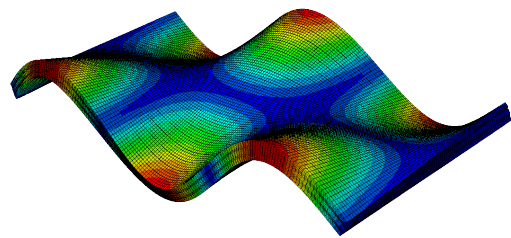
(h) Mode shape of the eighth eigenfrequency, at the frequency 78.506 Hz.

Figure 5.4: The first eight mode shapes of the CLT floor. The largest mesh element is $0.0375 \times 0.0375 \times 0.01$ m^3.

5.4 3D-model with separate layers

A solid block with the dimensions $6 \times 3 \times 0.2$ m^3 is created as the base for this model. Four partitions are then assigned, creating five equally thick layers of the solid body. The material orientation of the second and fourth layer are rotated 90-degrees around the z-axis. The 3D floor model with separated layers are shown in Figure 5.5.
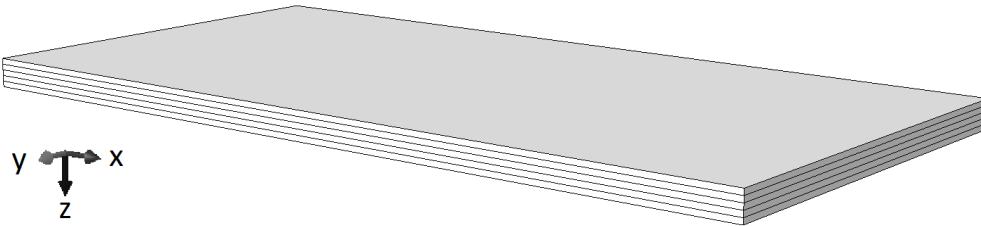
Figure 5.5: The floor modelled as a 3D part with five separate layers. The global coordinate system is given.

The engineering constants and density assigned to the *3D-model with separate layers* are given in Table 5.4. Engineering Constants are selected in Abaqus.

Table 5.4: Local stiffness parameters and Poisson's ratios used. All stiffness parameters are expressed in MPa, Poisson's ratio is unitless and the density is expressed in kg/m^3.

E_1	E_2	E_3	ν_{12}	ν_{13}	ν_{23}	G_{12}	G_{13}	G_{23}	ρ
11 000	370	370	0.51	0.38	0.31	690	690	50	420

5.4.1 Mesh convergence study

The element convergence study is performed with the floor as simply supported on two opposite edges and two unsupported. The boundary conditions are located in the centre of the thickness direction of the floor element. The convergence study was performed with linear elements as well as quadratic elements. In the xy-plane the element side are set to: 1.2, 0.6, 0.3, 0.15, 0.075 and 0.0375 m. In the xy-plane, all four sides of the elements have the same length, with an exception to the largest mesh where the elements are 1.2 m $\times$ 1.0 m.

The first mesh convergence study, is performed with 20-node hexahedral elements using quadratic interpolation and full integration (C3D20), in Abaqus. The results of the convergence study of the first eight eigenfrequencies are shown in Figure 5.6. The thickness of the internal layers is divided into one, two, three and lastly four separate elements, respectively, which result in a total of 5, 10, 15 and 20 elements of the thickness direction of the model.

The linear study is performed with 8-node hexahedral elements using linear interpolation and full integration (C3D8). Each layer of laminations is divided into two parts and then into four parts per layer, which results in a total of 10 and 20 element layers, respectively. Due to the requirement of placing the boundary conditions in the centre of the thickness only even numbers may be used for the analysis with linear elements. The results of the convergence study of the first eight eigenfrequencies are shown in Figure 5.7.

5.4.2   Eigenfrequencies and mode shapes

The eigenfrequencies from assigning quadratic elements to the model are shown in Table 5.5. Each layer of laminations are divided into one, two, three and four parts, respectively, which results in a total of 5, 10, 15 and 20 elements over the thickness. The results from the finest mesh are shown, with an elements side length of 0.0375 m.

Table 5.5: The eigenfrequencies of the *3D-model with separate layers* with an element side length of 0.0375 metres. Quadratic elements are used. The frequencies are expressed in Hz.

No. of Layers	$f_{n,1}$	$f_{n,2}$	$f_{n,3}$	$f_{n,4}$	$f_{n,5}$	$f_{n,6}$	$f_{n,7}$	$f_{n,8}$
5	11.005	16.229	38.914	44.237	56.350	74.546	75.177	80.025
10	11.005	16.231	38.921	44.248	56.351	74.558	75.200	80.055
15	10.989	16.172	38.742	43.988	56.276	74.218	74.618	79.374
20	11.005	16.229	38.916	44.241	56.348	74.549	75.186	80.038

The model with linear elements is analysed where each internal layer is divided into two parts and four parts, respectively, which results in a total of 10 and 20 elements in the thickness direction of the model. In Table 5.6 the eigenfrequencies calculated for the models with linear elements and a mesh size in the xy-plane of 0.0375 m $\times$ 0.0375 m are shown.

Table 5.6: The eigenfrequencies of the *3D-model with separate layers* with an element side length of 0.0375 m. Linear elements are used. The frequencies are expressed in Hz.

No. of Layers	$f_{n,1}$	$f_{n,2}$	$f_{n,3}$	$f_{n,4}$	$f_{n,5}$	$f_{n,6}$	$f_{n,7}$	$f_{n,8}$
10	11.000	16.242	38.916	44.266	56.228	74.458	75.207	80.085
20	11.015	16.249	38.983	44.322	56.406	74.649	75.380	80.242

The corresponding mode shapes to the model with the finest mesh with quadratic elements are given in Figure 5.8. The eigenfrequencies calculated are given in the caption of each subfigure. The first, thrid and seventh mode shapes corresponds to the first, second and third bending mode, respectively. The second mode shape corresponds to the first torsional mode. The fourth, fifth, sixth and eighth mode shapes includes torsion.
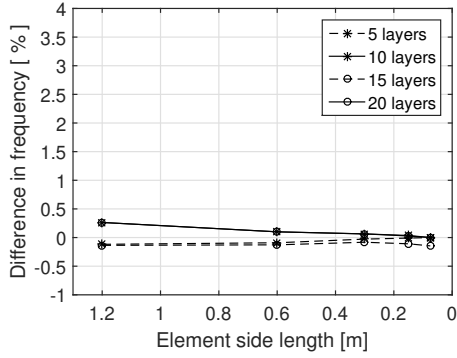
(a) The first eigenfrequency.
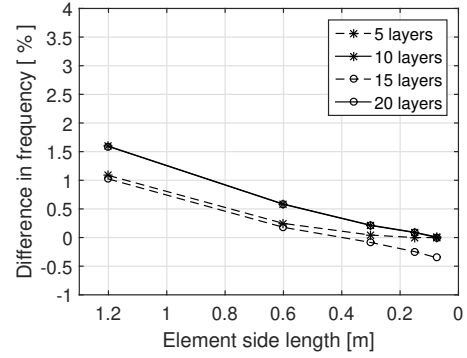
(b) The second eigenfrequency.
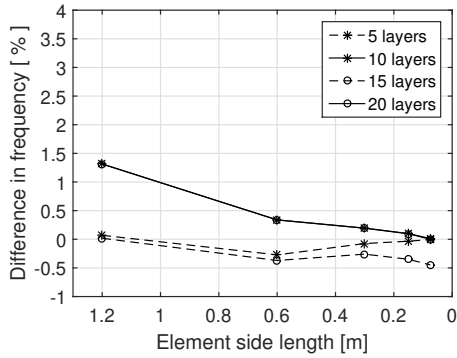
(c) The third eigenfrequency.
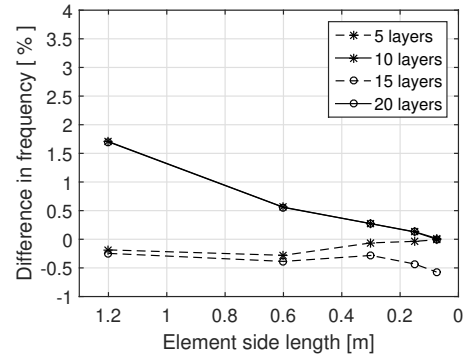
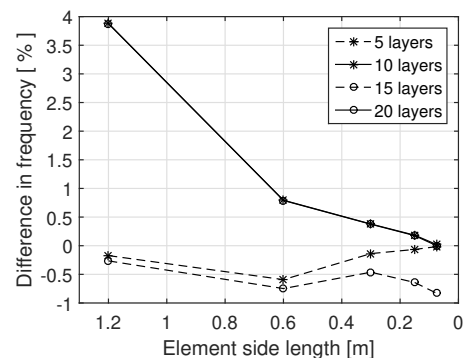**(d)** The fourth eigenfrequency.
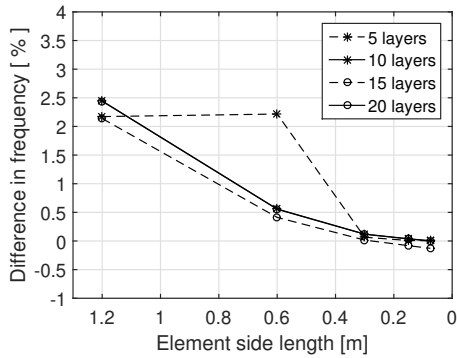
(e) The fifth eigenfrequency.

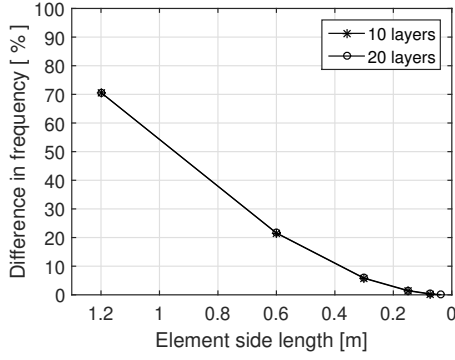

(f) The sixth eigenfrequency.
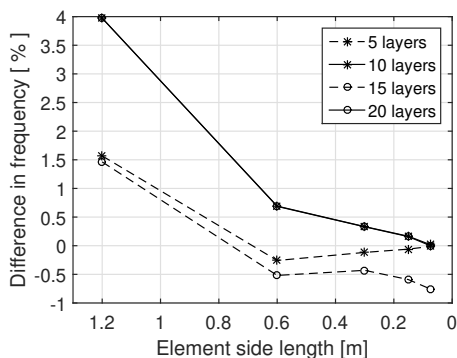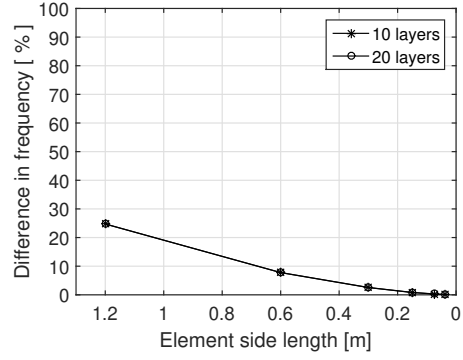

(g) The seventh eigenfrequency.
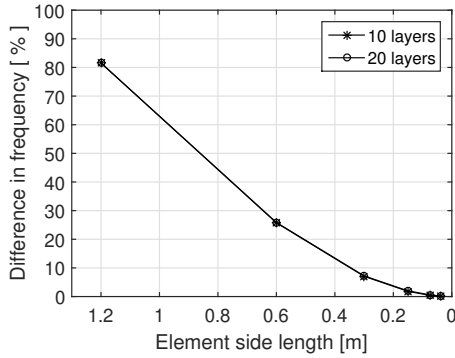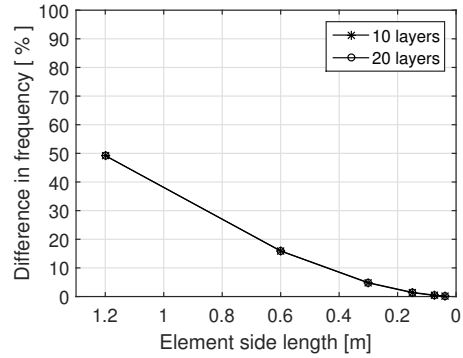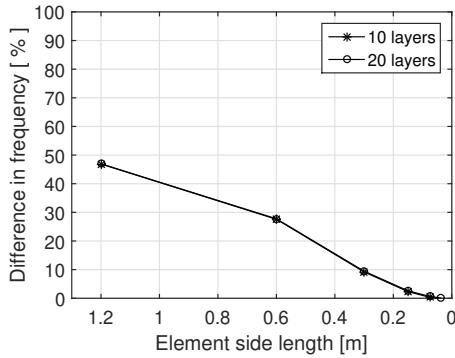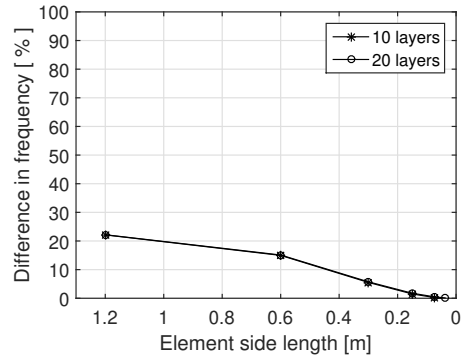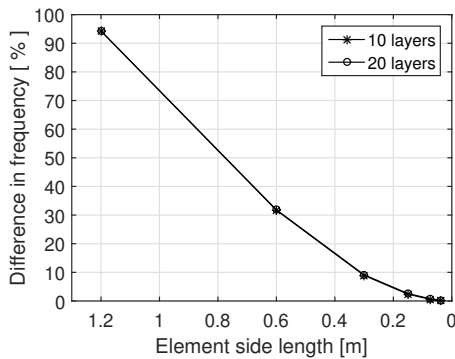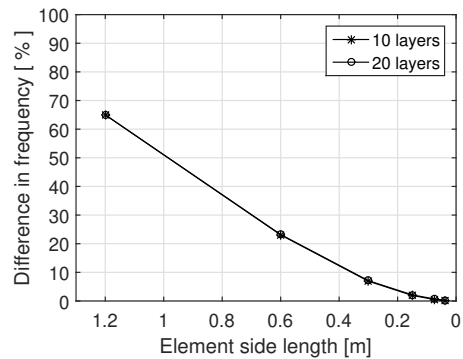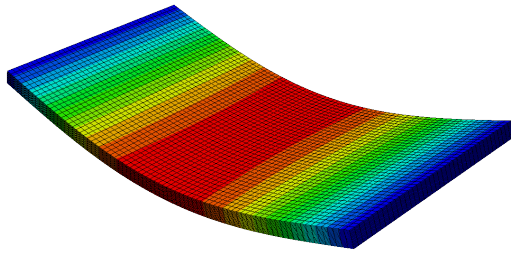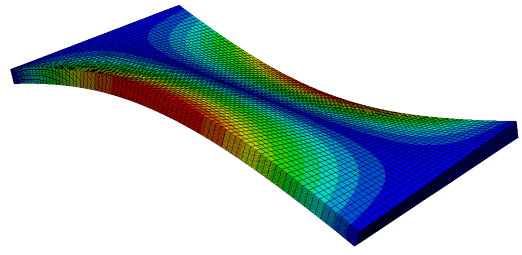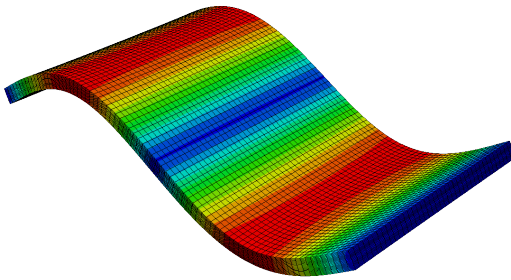

(h) The eighth eigenfrequency.

Figure 5.6: Convergence study of the first eight eigenfrequencies, with quadratic elements. The element side length is shown on the horizontal axis. The difference in frequency expressed in percent is shown on vertical axis. The reference frequencies is chosen as the eigenfrequencies of the finest mesh of the quadratic analysis.

(a) The first eigenfrequency.

(b) The second eigenfrequency.

(c) The third eigenfrequency.

(d) The fourth eigenfrequency.

(e) The fifth eigenfrequency.

(f) The sixth eigenfrequency.

(g) The seventh eigenfrequency.

(h) The eighth eigenfrequency.

Figure 5.7: Convergence study of the first eight eigenfrequencies, with linear elements. The element side length is shown on the horizontal axis. The difference in frequency expressed in percent is shown on the vertical axis. The reference eigenfrequencies are given by the model with quadratic elements and with the finest mesh, 0.0375 m^2 and the total thickness of the floor divided into 20 layers.

(a) Mode shape of the first eigenfrequency, at the frequency 11.005 Hz.

(b) Mode shape of the second eigenfrequency, at the frequency 16.229 Hz.

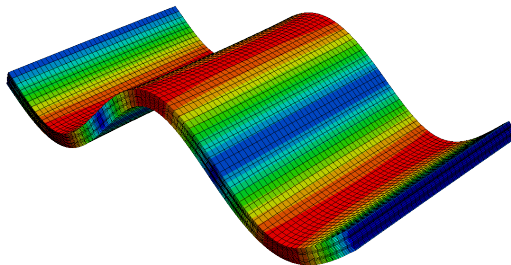(c) Mode shape of the third eigenfrequency, at the frequency 38.916 Hz.
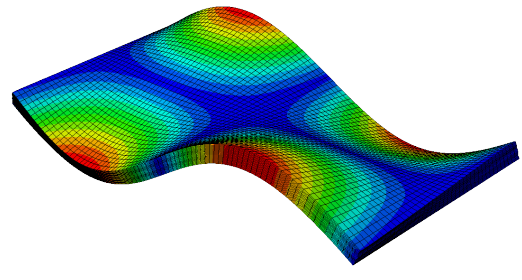
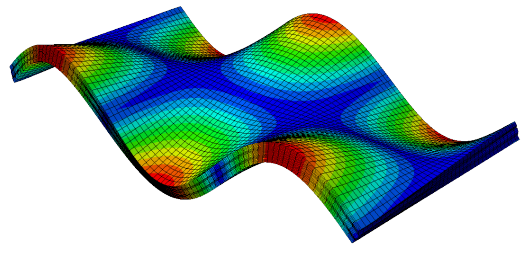(d) Mode shape of the fourth eigenfrequency, at the frequency 44.241 Hz.
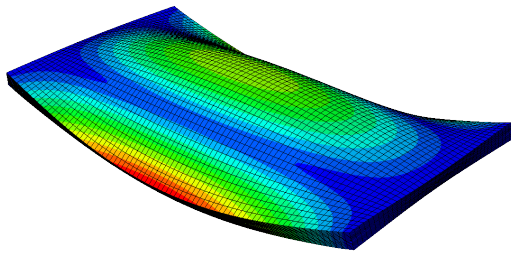
(e) Mode shape of the fifth eigenfrequency, at the frequency 56.348 Hz.
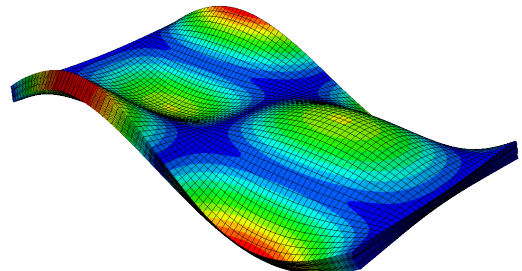
(f) Mode shape of the sixth eigenfrequency, at the frequency 74.549 Hz.

(g) Mode shape of the seventh eigenfrequency, at the frequency 75.186 Hz.

(h) Mode shape of the eighth eigenfrequency, at the frequency 80.038 Hz.

Figure 5.8: The first eight mode shapes of the CLT floor. The model has an element size of 0.0375×0.0375 m^2 in the xy-plane and each ply of laminations are divided into four equal layers.

5.4.3   Stiffness parameters modified with Gamma-method

The FE model is designed with five layers of laminations, in order to simplify the model without removing the layered design, it might be possible to reduce the number of stiffness parameters assigned to the model. The orthotropic material will be replaced with an isotropic representation, based on the Gamma-method in Section 2.3.2. Depending on the grain direction of the laminations in the layers, two different isotropic materials will be assigned.

When a CLT floor is analysed accordingly to beam theory, the second moment of inertia should be reduced due to the connections between the internal layers of laminations. In Section 4.3.1 an effective second moment of inertia is calculated for the CLT floor: $I_{ef.l} = 0.0014488$ m^4. The effective second moment of inertia is calculated around the global x-axis, which result in $I_{ef.b} = 0.0006181$ m^4.

In Abaqus, the second moment of inertia is calculated from the geometry of the model. To include a similar reduction as to the 1D model, a reduction to the stiffness parameters has to be made. The second moment of inertia of a rectangular cross-section is given by:

$$I = \frac{bh^3}{12} \tag{5.2}$$

The dimensions of the model that are used to calculate the second moment of inertia around the two axis are the height (h) of 0.2 m and the width (b) of 3 m and the length (l) of 6 m, which results in:

$$I_{model.l} = 0.0020 \text{ m}^4$$
$$I_{model.b} = 0.0040 \text{ m}^4$$

The bending stiffness (EI) should be equal between the two models. Therefore, ψ_x is introduced as a reduction factor to the bending stiffness of the FE model:

$$\psi_x I_{model.x} E = I_{ef.x} E \tag{5.3}$$

Young's modulus is the same for both sides of the equation, which leave us with the difference of the second moment of inertia. The ψ_x-factor can then be calculated as:

$$\psi_x = \frac{I_{ef.x}}{I_{model.x}} \tag{5.4}$$

The ψ_x-factor is calculated for the two stiffness directions, with the parameters given above:

$$\psi_l \approx 0.724$$
$$\psi_b \approx 0.155$$

Two isotropic material properties are produced and assigned to the layers depending on the local material orientation of the layers. The factors are multiplied with the Young's modulus in the local main direction (E_1). The first, third and fifth layer

are modified with ψ_l, which gives $E = 7\,964$ MPa. The second and fourth layer is modified with ψ_b which gives $E = 1\,705$ MPa. Poisson's ratio is chosen as 0.3 in both cases. The eigenfrequencies of the reduced material properties are given in Table 5.7, the modes shown are the ones comparable to the modes of the *3D-model with internal laminations*, see Figure 5.4.

Table 5.7: Eigenfrequencies of the model with modified stiffness parameters. The isotropic material parameters in the first, third and fifth layer is $E = 7\,964$ MPa and the second and fourth layer is selected as $E = 1\,705$ MPa. $\nu = 0.3$ for all layers. The eigenfrequencies are expressed in Hz.

$f_{n,1}$	$f_{n,2}$	$f_{n,3}$	$f_{n,4}$	$f_{n,5}$	$f_{n,6}$	$f_{n,7}$	$f_{n,8}$
10.077	27.407	40.279	64.442	106.72	143.45	89.511	115.78

5.5   2D composite model

The model is created as a 6 m × 3 m plate with a thickness of 0.2 m. The material properties are assigned for a composite layup in Abaqus. A conventional shell is assigned and the different layers are assigned properties through five different plies. The model and the ply plot is shown in Figure 5.9. Rotation and displacements DOFs are available through the conventional shell.
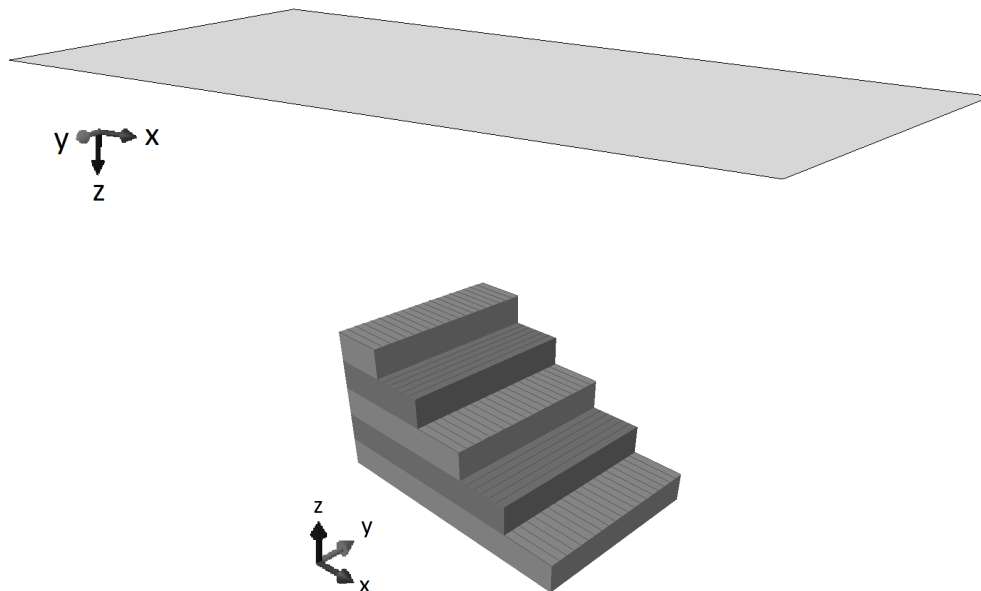

Figure 5.9: Above, the 2D model of the floor. Below, is the ply stack of the floor. Each ply has a height of 40 mm and the material orientation is visualized by the lines on top of each ply. The global coordinate system is shown in relation to both pictures.

The material properties are assigned to the model through the option *Lamina*. The following stiffness parameters are required as input to perform the analysis; E_1, E_2,

ν_{12}, G_{12}, G_{13} and G_{23}. The last two parameters are included because they may be used for modelling transverse shear deformation in a shell (*Abaqus Analysis User's Manual* 2006). The material parameters used are given in Table 5.8.

Table 5.8: The local stiffness parameters, Poisson's ratio and density assigned to the *2D composite model*. All stiffness parameters are expressed in MPa, Poisson's ratio is unitless and the density is expressed in kg/m^3.

E_1	E_2	ν_{12}	G_{12}	G_{13}	G_{23}	ρ
11 000	370	0.51	690	690	50	420

5.5.1 Mesh convergence study

The element convergence study is performed with the floor as simply supported. The boundary conditions is specified at the reference surface. On one of the sides of the span, the displacements are prescribed in the x-direction and z-direction, one endpoint of that edge is prescribed in the y-direction. On the other side of the span, the z-direction along the edge and the y-direction of the corresponding endpoint to the other side are prescribed of displacements.

The convergence study is performed with linear and quadratic elements, respectively. 4-node shell elements with linear interpolation and full integration (S4) is selected in Abaqus for the linear analysis. The quadratic analysis is performed with 8-node shell element with using quadratic approimation and reduced integration (S8R). The convergence study of the first eight eigenfrequencies is shown in Figure 5.10. In the xy-plane the element side length are set to: 1.2, 0.6, 0.3, 0.15, 0.075 and 0.0375 m. All elements in the mesh have the same length of all four sides, with an exception to the largest element size where the elements are 1.2 m × 1.0 m. The reference frequencies are computed with the finest mesh and using quadratic elements.

5.5.2 Eigenfrequencies and mode shapes

The resulting eigenfrequencies of the model with linear and quadratic elements are shown in Table 5.9. The values are shown for the finest mesh, 0.0375 m × 0.0375 m.

Table 5.9: The eigenfrequencies for the linear and quadratic *2D composite model*. The frequencies are given in Hz.

| Element type	$f_{n,1}$	$f_{n,2}$	$f_{n,3}$	$f_{n,4}$	$f_{n,5}$	$f_{n,6}$	$f_{n,7}$	$f_{n,8}$
Linear	11.016	16.098	38.985	44.123	55.797	73.483	75.177	79.799
Quadratic	11.016	16.097	38.979	44.117	55.784	73.469	75.155	79.779

The mode shapes and the corresponding eigenfrequencies of each mode is displayed in Figure 5.11. The model with the finest mesh and quadratic elements is used. The first, thrid and seventh mode shapes corresponds to the first, second and third bending mode, respectively. The second mode shape corresponds to the first torsional mode. The fourth, fifth, sixth and eighth mode shapes includes torsion.
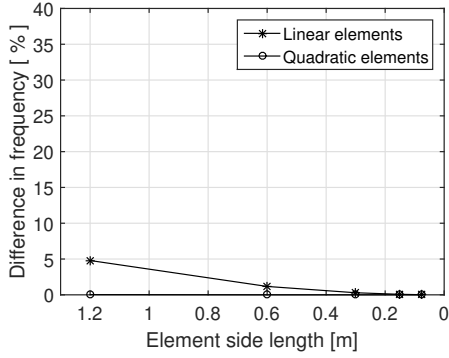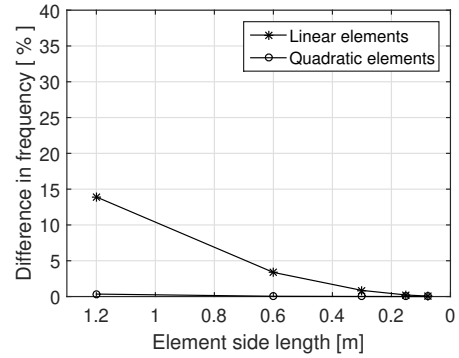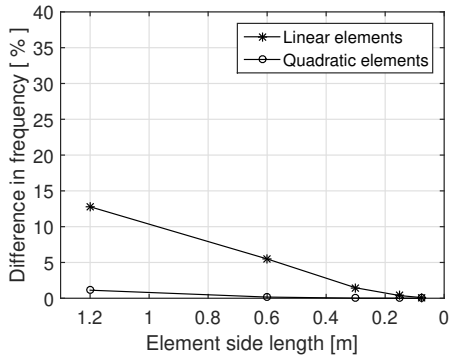
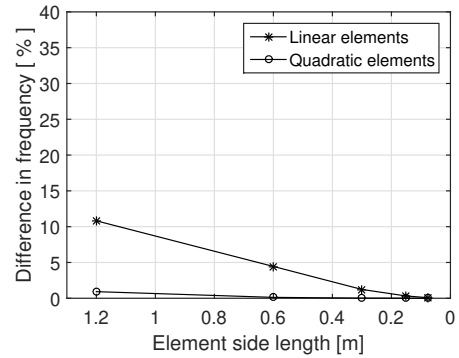**(a)** The first eigenfrequency.
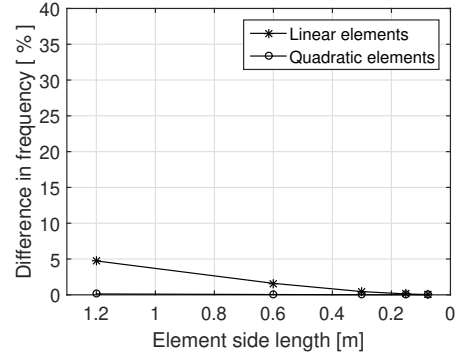
(b) The second eigenfrequency.
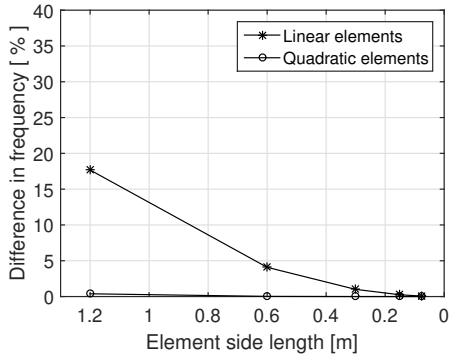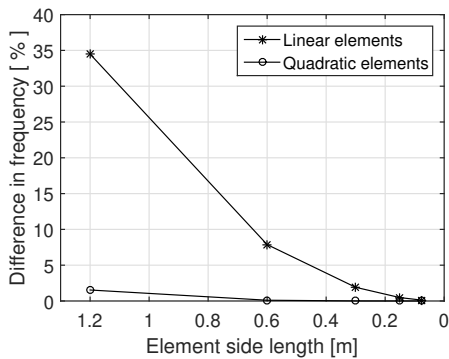
(c) The third eigenfrequency.
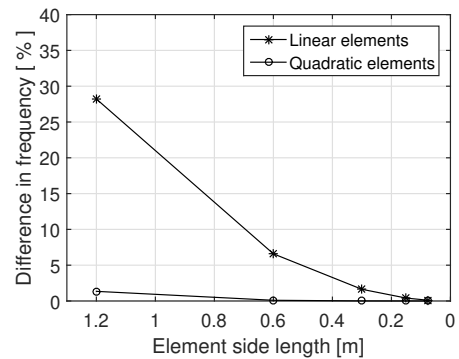
(d) The fourth eigenfrequency.

(e) The fifth eigenfrequency.

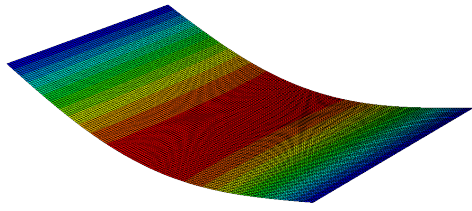**(f)** The sixth eigenfrequency.
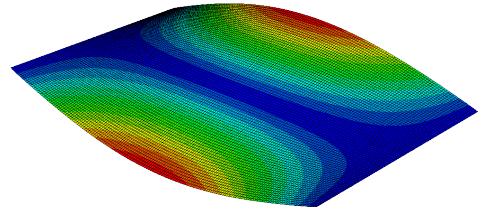
(g) The seventh eigenfrequency.
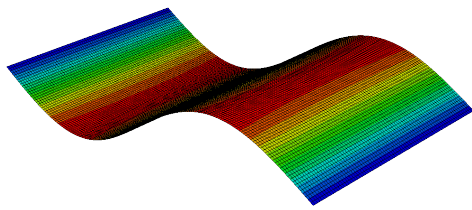
(h) The eighth eigenfrequency.

Figure 5.10: Convergence study of the first eight eigenfrequencies, with linear and quadratic elements. The element side length is shown on the horizontal axis. The difference of the frequency expressed in percent is shown on vertical axis. The reference frequencies are chosen as the model with the finest mesh and quadratic elements.
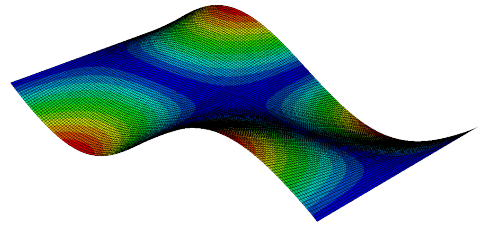
41

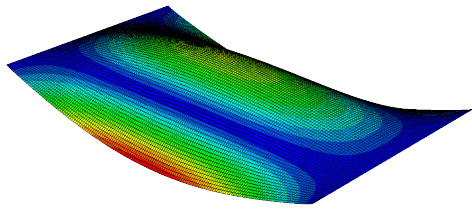**(a)** Mode shape of the first eigenfrequency, at the frequency 11.016 Hz.

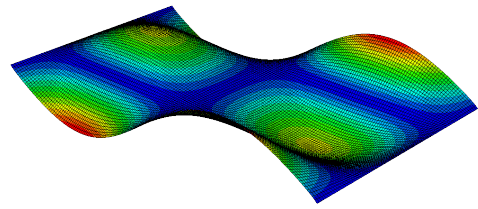**(b)** Mode shape of the second eigenfrequency, at the frequency 16.097 Hz.

(c) Mode shape of the third eigenfrequency, at the frequency 38.979 Hz.
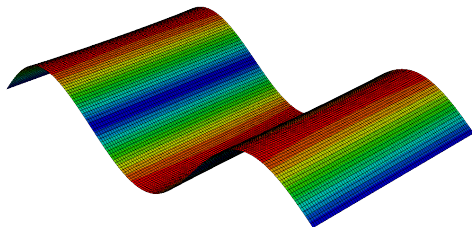
(d) Mode shape of the fourth eigenfrequency, at the frequency 44.117 Hz.

(e) Mode shape of the fifth eigenfrequency, at the frequency 55.784 Hz.

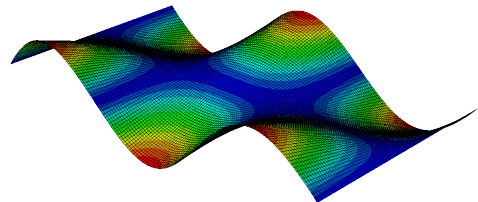**(f)** Mode shape of the sixth eigenfrequency, at the frequency 73.469 Hz.

(g) Mode shape of the seventh eigenfrequency, at the frequency 75.115 Hz.

(h) Mode shape of the eighth eigenfrequency, at the frequency 79.779 Hz.

Figure 5.11: The first eight mode shapes of the CLT floor. The model has an element size of 0.0375 m × 0.0375 m. The eigenfrequencies are given from the model using quadratic elements.

5.5.3 Stiffness parameters modified with Gamma-method

In order to simplify the FE model without removing the layered design, it might be possible to reduce the number of stiffness parameters assigned to the model. The orthotropic characteristics are reproduced as isotropic materials according to the Gamma-method, the same parameters are selected as for the *3D-model with separate layers*, see Section 5.4.3. Young's modulus of the first, third and fifth layer are set as $E = 7\ 964$ MPa and for the second and fourth layer, $E = 1\ 705$ MPa. Poisson's ratio is chosen as 0.3 in both cases. The eigenfrequencies of the reduced material properties are given in Table 5.10, the modes shown is the ones comparable to the modes of the *3D-model with internal laminations*, see Figure 5.4.

Table 5.10: Eigenfrequencies of the model with modified stiffness parameters. The isotropic material parameters in the first, third and fifth layer is $E = 7\ 964$ MPa and $\nu = 0.3$. The second layer and fourth is selected as $E = 1\ 705$ MPa and $\nu = 0.3$. The eigenfrequencies are expressed in Hz.

1st	2nd	3rd	4th	5th	6th	7th	8th
10.078	27.435	40.395	64.505	106.76	143.59	89.578	115.91

5.6 2D plate model

The same base is used for this model as for *2D composite model*. The model is created as a 6 m × 3 m plate with a thickness of 0.2 m, see Figure 5.12.
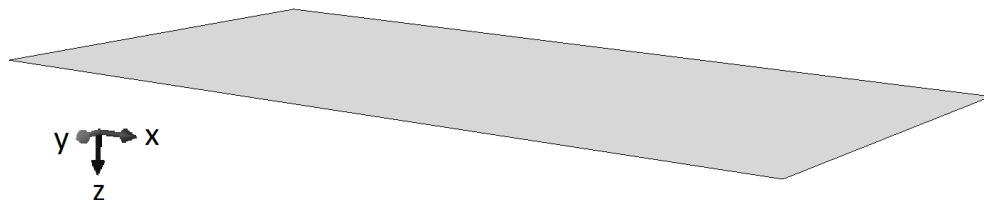

Figure 5.12: The *2D plate model*. The global coordinate system is given.

Stiffness parameters assigned to this model is given in Table 5.11. The model is 2D which implies that E_3, ν_{13} and ν_{23} are not required for the analysis (*Abaqus Analysis User's Manual* 2006). The material parameters are assigned to the model with the option *Lamina*.

5.6.1 Mesh convergence study

The mesh convergence study is performed with 4-node shell elements with linear interpolation and full integration (S4). The model is analysed according to plate theory which results in that the elements are 2D, in the *xy*-plane. The convergence study is

Table 5.11: Stiffness parameters, Poisson's ratio and density assigned for the *2D plate model*. All stiffness parameters are expressed in MPa, Poisson's ratio is unitless and the density is expressed in kg/m^3.

E_1	E_2	ν_{12}	G_{12}	G_{13}	G_{23}	ρ
11 000	370	0.51	690	690	50	420

performed with a mesh grid where all the elements four sides have the same length, with an exception to the largest element mesh size where the elements are 1.2 m × 1.0 m. The side lengths of the elements are then chosen as: 0.6, 0.3, 0.15, 0.075 and 0.0375 m. The convergence study is performed by analysing the value of the first eight eigenfrequencies. The reference value for each convergence is chosen as the eigenfrequency of the finest mesh, 0.0375 m^2. The results of the mesh convergence study of the first eight eigenfrequencies are plotted in Figure 5.13.

5.6.2 Eigenfrequencies and mode shapes

The eigenfrequencies completed with the model using linear elements are shown in Table 5.12. The values are shown for the finest mesh, 0.0375 × 0.0375 m^2.

Table 5.12: The eigenfrequencies for the linear and *2D plate model*. The frequencies are given in Hz.

| Element type	$f_{n,1}$	$f_{n,2}$	$f_{n,3}$	$f_{n,4}$	$f_{n,5}$	$f_{n,6}$	$f_{n,7}$	$f_{n,8}$
Linear	12.801	17.829	34.749	49.924	55.112	65.893	71.283	99.164

The corresponding mode shapes to the first eight eigenfrequencies are given in Figure 5.14. The frequencies are given in the caption of each mode shape. The first, thrid and seventh mode shapes corresponds to the first and fourth bending mode, respectively. The second mode shape corresponds to the first torsional mode. The third, fifth, sixth, seventh and eighth mode shapes includes torsion.
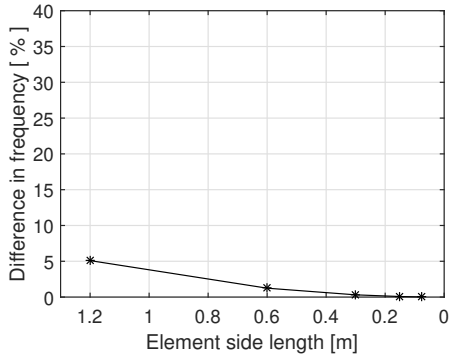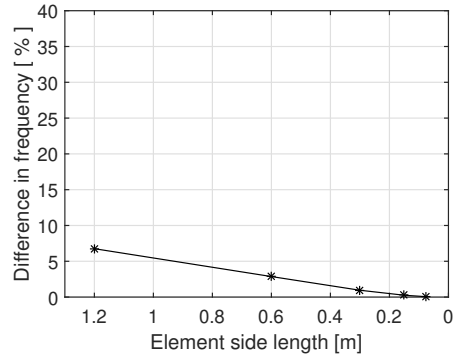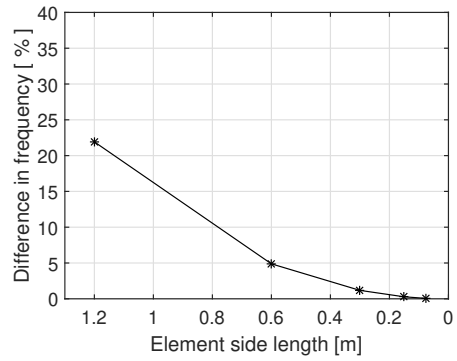
(a) The first eigenfrequency.

(b) The second eigenfrequency.
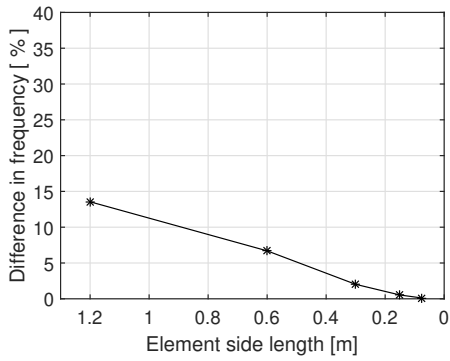
(c) The third eigenfrequency.

(d) The fourth eigenfrequency.
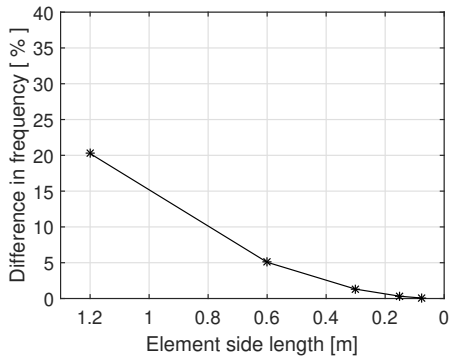
(e) The fifth eigenfrequency.
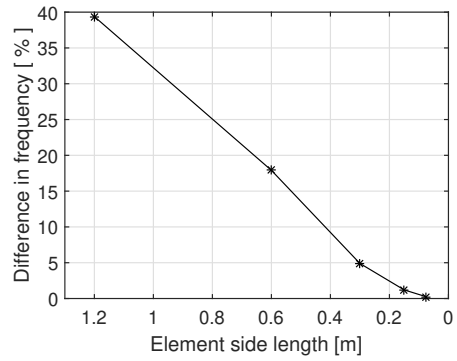
(f) The sixth eigenfrequency.
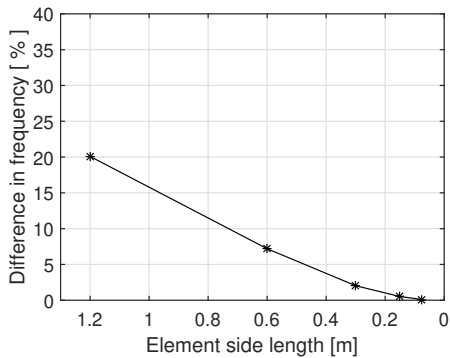
(g) The seventh eigenfrequency.
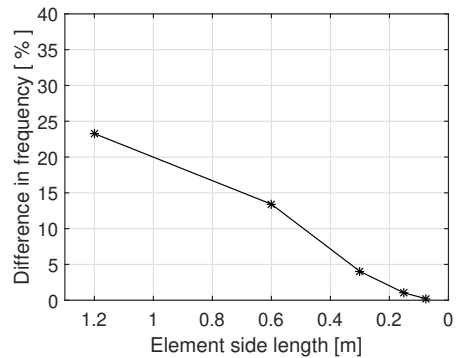
(h) The eighth eigenfrequency.

Figure 5.13: Convergence study of the first eight eigenfrequencies, performed with linear elements. The element side length is shown on the horizontal axis. The difference between the reference frequency and the corresponding frequency to the mesh size is expressed in percent and shown on vertical axis.

45
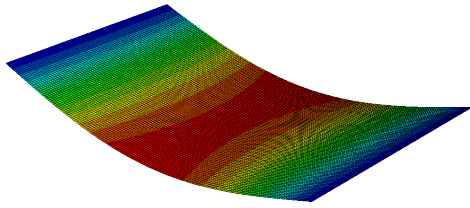
(a) Mode shape of the first eigenfrequency, at the frequency 12.801 Hz.
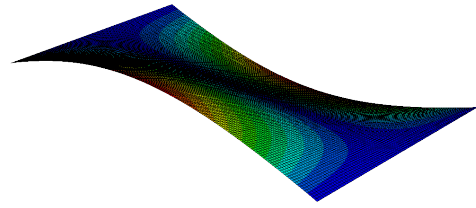
(b) Mode shape of the second eigenfrequency, at the frequency 17.829 Hz.
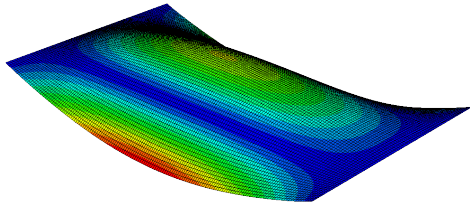
(c) Mode shape of the third eigenfrequency, at the frequency 34.749 Hz.
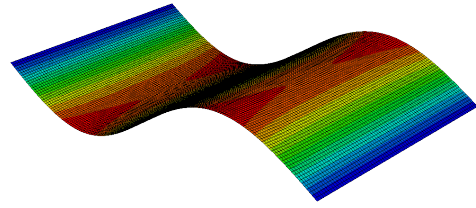
(d) Mode shape of the fourth eigenfrequency, at the frequency 49.924 Hz.
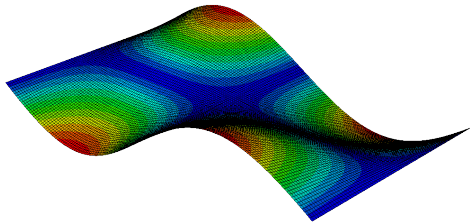
(e) Mode shape of the fifth eigenfrequency, at the frequency 55.112 Hz.
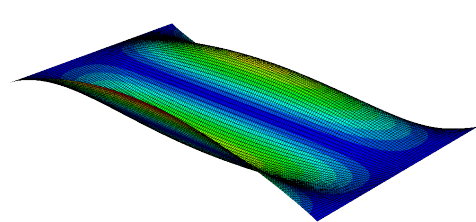
(f) Mode shape of the sixth eigenfrequency, at the frequency 65.893 Hz.
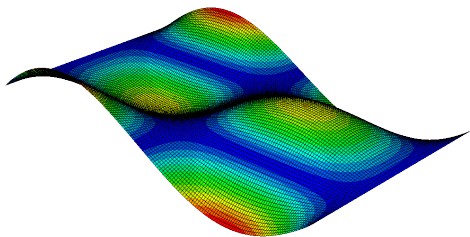
(g) Mode shape of the seventh eigenfrequency, at the frequency 71.283 Hz.
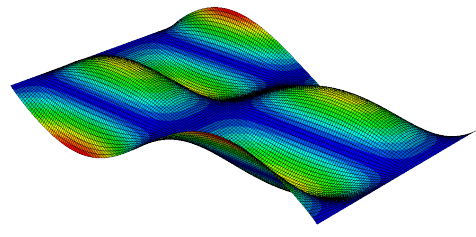
(h) Mode shape of the eighth eigenfrequency, at the frequency 99.164 Hz.

Figure 5.14: The first eight mode shapes of the CLT floor. The model has a mesh size of 0.0375×0.0375 m^2. Linear elements are used.

5.6.3 Stiffness parameters modified with Gamma-method

Two different materials are produced to try to mimic the behaviour of the orthotropic characteristics; one isotropic and one orthotropic modified with the gamma-factors calculated in Section 5.4.3. The isotropic material involve a reduced Young's modulus, $E = 7\,964$ MPa and with a Poisson's ratio of 0.3. The orthotropic material are given the material parameters $E_1 = 7\,964$ MPa, $E_2 = 1\,705$ MPa, the other parameters are left unchanged. The eigenfrequencies of the reduced material properties are given in Table 5.13, the modes selected are the ones comparable to the modes of the *3D-model with internal laminations*, see Figure 5.4.

Table 5.13: Eigenfrequencies of the models with modified stiffness parameters. The isotropic analysis is performed with $E = 7\,964$ MPa and $\nu = 0.3$.
$E_1 = 7\,964$ MPa, $E_2 = 1\,705$ MPa and the rest engineering constant are kept the same as earlier for the orthotropic material. The eigenfrequencies are expressed in Hz.

Material property	$f_{n,1}$	$f_{n,2}$	$f_{n,3}$	$f_{n,4}$	$f_{n,5}$	$f_{n,6}$	$f_{n,7}$	$f_{n,8}$
Isotropic	11.047	30.714	44.446	72.281	118.96	162.24	99.733	130.57
Orthotropic	10.951	16.700	43.208	49.484	50.940	77.615	94.518	100.15

The isotropic representation in Table 5.13 is only able to reproduce a similar prediction of the first eigenfrequency. Even though the stiffness is reduced in the grain direction with the ψ-factors, the stiffness in the other directions are increased with a significant number, which probably is the reason why the other eigenfrecuencies are higher. The orthotropic representation results in a more accurate prediction of the eigenfrequencies, but as the frequencies increases with higher modes, the difference between the orthotropic representation and the reference model (*3D-model with internal laminations*) increases.

5.7 Summary of the results

In Table 5.14 the eigenfrequencies of the different models are given for the finest mesh of each model. The modes given are those comparable to the mode shapes of the *3D-model with internal laminations*, see Figure 5.4. The models with modified stiffness parameters are followed by ψ, both for the isotropic (iso) and orthotropic (ortho) parameters.

Table 5.14: Eigenfrequencies for the finest mesh of the models are presented. The models with modified stiffness parameters are followed by ψ. The frequencies are given in Hz.

Model	$f_{n,1}$	$f_{n,2}$	$f_{n,3}$	$f_{n,4}$	$f_{n,5}$	$f_{n,6}$	$f_{n,7}$	$f_{n,8}$
2D plate ortho	12.801	17.829	49.924	55.112	34.749	71.283	107.87	112.58
2D plate iso ψ	11.047	30.714	44.446	72.281	118.96	162.24	99.733	130.57
2D plate ortho ψ	10.951	16.700	43.208	49.484	50.940	77.615	94.518	100.15
2D composite	11.016	16.097	38.979	44.117	55.784	73.469	75.155	79.779
2D composite iso ψ	10.078	27.435	40.395	64.505	106.76	143.59	89.578	115.91
3D layers	11.005	16.229	38.916	44.241	56.348	74.549	75.186	80.038
3D layers iso ψ	10.077	27.407	40.279	64.442	106.72	143.45	89.511	115.78
3D laminations	10.950	14.968	38.751	42.717	53.194	70.206	74.929	78.506

The model which should be most accurate is the *3D-model with internal laminations* with the finest mesh size, this model is chosen as reference. In Table 5.15, the difference in percentage of the eigenfrequencies in comparison to the reference model is given.

Table 5.15: The difference expressed in percent of the eigenfrequencies in relation to the *3D-model with internal laminations* with the finest mesh. The models with modified stiffness parameters are followed by ψ.

Model	$f_{n,1}$	$f_{n,2}$	$f_{n,3}$	$f_{n,4}$	$f_{n,5}$	$f_{n,6}$	$f_{n,7}$	$f_{n,8}$
2D plate ortho	16.9	19.1	28.8	29.0	34.7	1.5	44.0	43.4
2D plate iso ψ	0.9	105.2	14.7	69.2	123.6	131.1	33.1	66.3
2D plate ortho ψ	0.01	11.6	11.5	15.8	4.2	10.6	26.1	27.6
2D composite	0.6	7.5	0.6	3.3	4.9	4.7	0.3	1.6
2D composite iso ψ	8.0	83.3	4.2	51.0	100.7	104.5	19.6	47.6
3D layers	0.5	8.4	0.4	3.6	5.9	6.2	0.3	2.0
3D layers iso ψ	8.0	83.1	3.9	50.9	100.6	104.3	19.5	47.5

6 Discussion

The most accurate FE model (*3D-model with internal laminations*) of a CLT floor slab is selected as reference when comparing the models with different levels of detail. This is reasonable due to the fact that it has most features in common with a real CLT floor. A result of meshing the reference model, which have a 0.2 mm spacing between the laminations, is that the aspect ratio of some elements become large. The aspect ratio is the ratio between the longest and shortest edge of an element (*Abaqus/CAE User's Manual* 2010). In this case, to keep a reasonable aspect ratio, the other side lengths of these elements should be about 0.004 m and the finest mesh analysed is 0.0375 m. This may have an impact on the results, but because no error occurs throughout the analyses and the other models converge towards similar values this influence is assumed to be negligible.

The choice of element type is favourable to quadratic elements when comparing the required mesh size in the horizontal plane (*xy*-plane), see Figures 5.10, 5.7 and 5.6. Quadratic elements are not analysed for the *3D-model with internal laminations* due to the computational cost required for the resulting number of DOFs, a similar behaviour to the other models can however be expected. The choice of quadratic elements results in relatively accurate frequencies in relation to the converged model. A difference less than five percent for both models with quadratic elements analysed with an element size of 1.2 m × 1.0 m, which in this case results in five elements in the length direction and three in the width direction. The same accuracy (a difference under 5 %) with linear elements is achieved with an element mesh size of 0.3 m × 0.3 m in the horizontal plane, which results in 20 elements in the length direction and 10 in the width direction.

The number of elements in the thickness direction of the floor slab does not influence the eigenfrequencies substantially, see Figure 5.6. The minimum number of elements possible in accordance with the modelling choice is equal to the number of plies of the floor (five), and at most 20 layers are used. Five elements are therefore considered sufficient to capture the behaviour to simulate the eigenfrequencies. It might be possible that fewer element would result in less accuracy but due to the assemblage of the models, it cannot be analysed in this investigation.

In Figure 5.6 some unexpected behaviour can be noticed when 15 elements are used in the thickness direction of the floor slab. The model converges toward a lower frequency than for all the other number of elements for all modal frequencies. If smaller elements would have been analysed it might converge towards the same value but no apparent reason why this behaviour appear is known to the author.

Mimic the modal behaviour of the orthotropic material with an isotropic representation seems unsatisfactory, the models results in significant errors. The isotropic models should therefore not be employed, with an exception to the *2D plate model* if an evaluation of the fundamental frequency exclusively is of interest. This has also been shown by Ussher et al. (2017). The laminations in a CLT floor should be considered

as orthotropic during a eigenfrequency analysis.

In Table 5.15 it can be seen that the model that best represents the reference model is the *2D composite model*. The *3D-model with separate layers* which should be more accurate according to the level of detail only have more accuracy in the two first bending modes (modes 1 and 3). Although, the difference in frequency between these two models is relatively small, at most the difference in frequency between these two when compared to the reference model is 1.6 %, which result in that both models should be employable. Both models are constructed with five layers with the same material properties, the only difference is the analysis method.

The analysis of the fundamental frequency according to beam theory in Chapter 4.3 results in a frequency of 10.973 Hz. In comparison to the first eigenfrequency of the reference model (*3D-model with internal laminations*) at 10.950 Hz the difference is remarkably small. All models are although able to capture the behaviour of the fundamental frequency depending on the material parameters assigned, see Table 5.15. The first eigenfrequency is the easiest to predict.

7 Concluding remarks

7.1 Main conclusions

The study presents an evaluation of the level of detail necessary for a FE model to predict the eigenfrequencies of a CLT floor. All FE models that include multiple plies and the orthotropic characteristics results in a similar modal response up to 80 Hz. The less advanced models, where the layered composition is simplified to one unit deviate significantly. The results produced in this dissertation contribute with information of some parameters that are of importance when analysing a CLT floor slab in modal response.

The main conclusions that should be considered and can be applied when a modal analysis is to be performed on a CLT floor are listed below. The conclusions are assumed for a CLT floor with similar properties to the floor analysed in this study; be of rectangular shape in the horizontal plane and be simply supported along two opposite edges and free to vibrate on the other two edges.

- If eigenfrequencies up to 80 Hz are to be analysed, the lamination layers and ortotropic characteristics must be accounted for. A 2D model may be employed as long as the orthotropic features and layered composition is modelled.

- If the fundamental frequency exclusively is to be estimated for a CLT floor, a simple 1D analysis is able to capture the modal response.

- Quadratic elements should be assigned to the model to reduce the computational cost.

7.2 Future work

A notation to this dissertation is that no confirmation of the actual mode shapes and natural frequencies have been executed. The investigation is only based on the numerical analysis performed. Validation of the behaviour by comparison with experimental data would be beneficial.

It would be of interest to further study how to model different construction joints, between multiple elements and supports, and determine how and if it would influence the dynamic response. According to Ussher et al. (2017) does these kinds of construction features significantly affect the dynamic response of lightweight structures as CLT. Some features and construction choices that may have a strong influence on the modes and eigenfrequencies may not have been included in this study.

The floor was analysed with no influence from non-structural elements, for example, human occupants, furniture, non-supporting walls etc. The floor analysed have a density of 420 kg/m^3 which result in a mass of 82 kg/m^2. An object located at the floor is likely to contribute to dynamic response; see, for example, Andersen (2019).

Bibliography

Abaqus Analysis User's Manual (2006). Version 6.6. Chap. 17.2.1 Linear Elastic Behavior.

Abaqus/CAE User's Manual (2010). Version 6.10. Chap. 17.6.1 Verifying your mesh.

Aicher, Simon and Gerhald Dill-Langer (2000). Basic considerations to rolling shear modulues in wooden boards, In: *Otto-Graf-Journal* 11.

Andersen, Lars, Christian Frier, Lars Pedersen, Peter Persson (2019). Influence of Furniture on the Modal Properties of Wooden Floors, In: *Model Validation and Uncertainty Quantification*, Volume 3, pp. 197–204.

Bathe, Klaus-Jürgen (2016). *Finite Element Procedures*, Second edition, Fouth printing, K.J. Bathe, Watertown, MA.

Bolmsvik, Åsa, Andreas Linderholt and Kirsi Jarnerö (2012). FE modeling of a lightweight structure with different junctions, In: *Proceedings of 9th Euronoise*, Prague, 10 – 13 June, 2012.

Bodig, Jozsef and Benjamin A. Jayne (1982). *Mechanics of Wood and Wood Composites*, Van Nostrand Reinhold Company Inc.

Borgström, Eric and Johan Fröbel (2017). *KL-trähandbok - Fakta och projektering av KL-träkonstruktioner*, Svenskt Trä.

Boverket (2016). *Boverkets konstruktionsregler*, EKS 10, ISBN tryck: 978-91-7563-327-5.

Chopra, Anil K. (2012). *Dynamics of structures - Theory and Applications to Earthquake Engineering*, Prentice Hall - Pearson Highered.

Dahl, Kristian B. (2009). *Mechanical properties of clear wood from Norway spruce*, PhD thesis, Norwegian University of Science and Technology.

Danielsson, Henrik (2013). *Perpendicular to grain fracture analysis of wooden structural elements - Models and Applications*, PhD thesis, LTH, Lund University.

EN 1995-1-1 (2004). *Eurocode 5 - Design of timber structures - Common rules and rules for buildings*, European Committee for Standardization.

EN 338 (2016). *Structural timber - strength classes*, European Committee for Standardization.

Fellmoser, Peter and Hans J. Blass (2004). Influence of rolling shear modulus on strength and stiffness of structural bonded timber elements, *Working Commission W18 - Timber Structures* 37, Edinburgh, United Kingdom, August, 2004.

Giang, Fanny and Ludmila Moroz (2013). *En jämförelse mellan två olika tröstomsystem och byggmetoder*, MA thesis, Royal Institute of Technology in Stockholm.

Green, David W., Jerrold E. Winandy and David E. Kretschmann (1999). Chap. 4 Mechanical Properties of Wood, *Wood Handbook - Wood as an Engineering Material*, United States Department of Agriculture.

ISO 10137 (2007). *Bases for design of structures - Serviceability of buildings and walkways against vibrations*, Second edition, International Organization for Standardization.

Johansson, Marie (2016). Chap. 2 - Structural properties of sawn timber and engineered wood products, *Design of timber structures - Structural aspects of timber construction*, Second edition, Vol. 1, Svenskt Trä.

European Commission (2019). *Major Concepts of the EN Eurocodes*, URL: https://euro-codes.jrc.ec.europa.eu/showpage.php?id=11 [2019-04-06].

Ottosen, Niels S. and Hans Petersson (1992). *Introduction to the Finite Element Method*. Harlow, England, Pearson Education Limited, ISBN: 0-13-473877-2.

Persson, Peter (2016). *Vibrations in Building Environment - Prediction and Reduction*, PhD thesis, LTH, Lund University.

Persson, Peter and Ola Flodén (2018). Towards uncertainty quantification of vibrations in wooden floors, In: *Proceedings of 25th International Congress on Sound and Vibration*, pp. 4254 – 4261, Hiroshima, Japan, July.

Persson, Peter and Ola Flodén (2019). Effect of material parameter variability on vibroacoustic response in wooden floors, *Applied Acoustics* 146, pp. 38–49.

Qian, Cheng, Sylvain Menard, Delphine Bard and Juan Negreira (2019). Development of a Vibroacoustic Stochastic Finite Element Prediction Tool for a CLT Floor, *Applied Sciences (Switzerland)* 9, 6, 1106.

Ussher, Ebenezer, Kaveh Arjomandi, Jan Weckendorf and Ian Smith (2017). Predicting effects of design variables on modal responses of CLT floors, *Structures* 11, pp. 40 – 48, DOI: 10.1016/j.istruc.2017.04.006.